NASA Author Manuscript
NASA Author Manuscript

Published in final edited form as:
J Guid Control Dyn. 2019 ; N/A: . doi:10.2514/1.G004556.

Theory of Fractional-Polynomial Powered Descent Guidance

Ping Lu[*]
San Diego State University, San Diego, California 92182-1308

Abstract

The notion and the theory of constructing planetary powered descent guidance laws based on fractional polynomials are introduced. Along the way a new perspective to the classical Apollo powered descent guidance designs is gained. As a foundation of this work, a theory is first developed on how to derive an explicit powered descent guidance law by selecting the feedback gains in a unique way in an implicit tracking guidance law. Then by employing a particular profile of the reference thrust acceleration in the tracking law with a special set of gains, a large family of powered descent guidance laws is obtained that offer the flexibility in trajectory shaping and thrust characteristics by two adjustable parameters. An equivalence theory is established to show that each in this family of guidance laws is actually the explicit guidance law from a fractional-polynomial thrust acceleration profile. This insight provides a perfect explanation to the predictable behavior and good targeting performance of these guidance laws. The well-known Apollo lunar descent guidance and E-guidance laws are revealed to be two members of this much broader class of fractional-polynomial powered descent guidance laws.

I. Introduction

The powered descent guidance system of a spacecraft is responsible for determining the required direction and magnitude of the engine thrust (or thrust acceleration) vector during a planetary descent and landing mission, so as to meet the required targeting condition at the end, such as that for touchdown at the designated landing site with the required velocity. This investigation was originally motivated by the desire to find the answers to several intriguing questions related to the augmented Apollo powered descent guidance (A^2PDG) law derived in a recent work by this author in Ref. [1]. The A^2PDG law unifies the two different Apollo-era powered descent guidance laws, the E-guidance in Ref. [2] and Apollo lunar descent guidance in Ref. [3, 4], preserving all the strengths of the Apollo powered descent guidance laws while offering the flexibility of tunability not available before. The A^2PDG law is constructed as follows: a linear function of time profile is used to define a reference thrust acceleration vector, and the corresponding reference velocity and position profiles are generated with with the specified targeting condition at the end; a feedback guidance law for the commanded thrust acceleration is then formed to track the reference profiles with two controller gains. When one of the gains is selected in a particular way, the A^2PDG law emerges that has a remaining adjustable gain, denoted by k_r. When $k_r = 6$, the guidance law becomes exactly the Apollo E-guidance law [2] which is based on a linear

[*]Professor and Chair, Department of Aerospace Engineering; plu@sdsu.edu, Fellow AIAA.

thrust acceleration profile. Yet when $k_r = 12$, the guidance law gives rise to the Apollo lunar descent guidance law [3, 4] which is designed by using a *quadratic* thrust acceleration profile. No explanation was available for the underlying reason of these phenomena at the time of preparation for Ref. [1]. The questions we set out to seek to answer in this work include:

i. Why do these remarkable results appear for $k_r = 6$ and $k_r = 12$ in the A^{2}PDG law?

ii. What does the A^{2}PDG law represent when the values of k_r are other than 6 and 12 – is there some inherent structure that links the E-guidance and Apollo lunar descent guidance at $k_r = 6$ and $k_r = 12$ as part of a continuous evolution when k_r varies?

iii. Why does the A^{2}PDG law have the excellent targeting performance and predictability for an arbitrary $k_r \geq 6$, notably better than a typical tracking law?

iv. Is there a broader and more general context, beyond the A^{2}PDG, in which other powered descent guidance laws exist that also share the similar insight provided by the answers to the above questions?

This search has not only successfully led to satisfying answers to all the above questions, but also the discovery of a large family of planetary powered descent guidance laws that offer significant flexibility in shaping the trajectory and guidance-command characteristics, while preserving the targeting accuracy.

Unlike a paper that is built on a substantial body of existing literature, there are few published papers which can be reviewed and directly contrasted to this work. However, the influence by and connection to the Apollo lunar descent guidance works are clear. In particular, the notion of parameterization of the thrust acceleration by a polynomial of time in Ref. [2] inspires the more general idea in this paper of representing the thrust acceleration by a linear combination of time-to-go with positive but not necessarily integer exponents. We call such a nonlinear function a fractional polynomial. The use of fractional polynomials plays the instrumental role in enabling the elegant results in this paper regarding the preceding questions (ii)–(iv).

The other key inspiration to this work is the tracking control formulation of the commanded thrust acceleration in Ref. [3]. This formulation offers an implicit guidance alternative to the explicit Apollo lunar descent guidance law. It is found in Ref. [3] that when each of the two tracking controller gains takes a particular value, the explicit and implicit versions of the guidance laws are identical, although no explanation or insight is available in Ref. [3] on the reason. This tracking guidance formulation is used to arrive at the tunable A^{2}PDG law in Ref. [1], and is central in the development in this paper. We will show that what is observed in Ref. [3] is not a coincidence, but a special case of a general property.

The classical Apollo lunar descent guidance law and E-guidance law will be shown to be just two members of the much larger class of fractional-polynomial powered descent guidance laws developed in this paper. The guidance laws in this family enjoy similar strengths, simplicity, and performance characteristics of the flight-proven Apollo lunar descent guidance law. Yet the availability of many more options in powered descent guidance laws to accommodate varying trajectory and guidance requirements is always welcomed, given the strong current interest in crewed landing missions on the Moon.

II. Explicit Guidance Laws from Implicit Formulation

The 3-dimensional equations of motion for powered descent dynamics over a planet (or the Moon) in vacuum can be expressed in a Cartesian coordinate system as

$$\dot{\boldsymbol{r}} = \boldsymbol{V} \tag{1}$$

$$\dot{\boldsymbol{V}} = \boldsymbol{g} + \boldsymbol{a}_T \tag{2}$$

where $\boldsymbol{r} \in R^3$ and $\boldsymbol{V} \in R^3$ are the position and velocity vector of the vehicle, and $\boldsymbol{g}$ the planetary gravitational acceleration vector which will be regarded as a constant vector in this paper. The thrust *acceleration* vector is $\boldsymbol{a}_T \in R^3$. The position and velocity $\boldsymbol{r}(t)$ and $\boldsymbol{V}(t)$ at the current time t are assumed to be known. Let $\boldsymbol{r}_f^* \in R^3$ and $\boldsymbol{V}_f^* \in R^3$ be the prescribed radius and velocity vectors at a specified final time $t_f \geq t$ that define the coordinates of the landing site and required touchdown velocity (direction and magnitude). The targeting condition is

$$\boldsymbol{r}\left(t_f\right) = \boldsymbol{r}_f^* \tag{3}$$

$$\boldsymbol{V}\left(t_f\right) = \boldsymbol{V}_f^* \tag{4}$$

Even though throughout this paper powered descent is the intended application, it is clear that the development in this paper is applicable to a more generic targeting problem in space flight where Eqs. (3) and (4) represent the desired final condition not necessarily meant for landing. The closed-loop guidance problem is to find the thrust acceleration command $\boldsymbol{a}_T(t)$ for every $t \leq t_f$ to steer the vehicle from the current state to the specified required targeting condition $(\boldsymbol{r}_f^*, \boldsymbol{V}_f^*)$ at the specified final time t_f.

In aerospace guidance, explicit guidance refers to an approach where the solution process works directly (i.e., explicitly) to meet the targeting condition each time when the guidance command is generated. Implicit guidance on the other hand indicates a method where the requirement of meeting the targeting condition is through an indirect association (i.e., implicitly), such as tracking a reference trajectory that satisfies the targeting condition. In this section a general technique is presented to derive an explicit guidance law for $\boldsymbol{a}_T$ by starting from an implicit guidance formulation. The ultimate value of this section however is to lay the groundwork for the development in Section III.

A. Two-Term Parameterization

At any current time $t \leq t_f$, define the time-to-go corresponding to a prescribed t_f by

$$t_{go} = t_f - t \tag{5}$$

Let $\phi_1(t_{go})$ and $\phi_2(t_{go})$ be two scalar integrable basis functions that one chooses. We seek to represent a reference thrust acceleration vector by

$$\boldsymbol{a}_d(t) = \boldsymbol{c}_1\phi_1\left(t_{go}\right) + \boldsymbol{c}_2\phi_2\left(t_{go}\right) \tag{6}$$

where $\boldsymbol{c}_1 \in R^3$ and $\boldsymbol{c}_2 \in R^3$ are constant vectors to be determined. Define

$$\bar{\phi}_i\left(t_{go}\right) = \int_{t_{go}}^{0} \phi_i(\tau)d\tau, \quad i = 1, 2 \tag{7}$$

$$\hat{\phi}_i\left(t_{go}\right) = \int_{t_{go}}^{0} \bar{\phi}_i(\tau)d\tau, \quad i = 1, 2 \tag{8}$$

Note that the integration is from t_{go} to 0. In actual time it is from the current instant t to the specified final time t_f. The only required condition on ϕ_1 and ϕ_2 is that

$$\Delta := \hat{\phi}_1\left(t_{go}\right)\bar{\phi}_2\left(t_{go}\right) - \hat{\phi}_2\left(t_{go}\right)\bar{\phi}_1\left(t_{go}\right) \neq 0, \ \forall t_{go} > 0 \tag{9}$$

This condition is to avoid a singularity in some of the equations in the subsequent development. It turns out that the condition in Eq. (9) is not even necessary for certain choices of ϕ_1 and ϕ_2. See for instance Section III-C. But we will make the assumption to facilitate a general discussion. Integrating Eqs. (1) and (2) backward with the above $\boldsymbol{a}_d$, and using the targeting conditions Eqs. (3) and (4) at $t = t_f$ (the beginning of the backward integration), we have the corresponding reference position and velocity profiles

$$\boldsymbol{r}_d(t) = \boldsymbol{r}_f^* + \boldsymbol{c}_1\hat{\phi}_1 + \boldsymbol{c}_2\hat{\phi}_2 - \boldsymbol{V}_f^* t_{go} + \frac{1}{2}\boldsymbol{g}t_{go}^2 \tag{10}$$

$$\boldsymbol{V}_d(t) = \boldsymbol{V}_f^* + \boldsymbol{c}_1\bar{\phi}_1 + \boldsymbol{c}_2\bar{\phi}_2 - \boldsymbol{g}t_{go} \tag{11}$$

where the argument of t_{go} in $\bar{\phi}$ and $\hat{\phi}_i$, $i = 1,2$, is dropped for brevity. Consider the guidance law for the commanded thrust acceleration from the following tracking controller

$$\boldsymbol{a}_T(t) = \boldsymbol{a}_d(t) - \beta_V\left(t_{go}\right)\left[\boldsymbol{V}(t) - \boldsymbol{V}_d(t)\right] - \beta_r\left(t_{go}\right)\left[\boldsymbol{r}(t) - \boldsymbol{r}_d(t)\right] \tag{12}$$

where the scalar feedback gains β_V and β_r may be dependent on t_{go}, and their forms are to be determined. Equation (12) generally represents an implicit guidance law because the objective of achieving the targeting condition is not explicit in the update of $\boldsymbol{a}_T(t)$, but implied by tracking a reference that meets the targeting condition. Substituting the expressions of $\boldsymbol{a}_d$, $\boldsymbol{V}_d$, and $\boldsymbol{r}_d$ into Eq. (12) and collecting the terms leads to

$$\begin{aligned}\boldsymbol{a}_T = \boldsymbol{c}_1\left(\phi_1 + \beta_V\bar{\phi}_1 + \beta_r\hat{\phi}_1\right) + \boldsymbol{c}_2\left(\phi_2 + \beta_V\bar{\phi}_2 + \beta_r\hat{\phi}_2\right) + \boldsymbol{g}t_{go}\left(\frac{1}{2}\beta_r t_{go} - \beta_V\right) \\ - \beta_V\left[\boldsymbol{V}(t) - \boldsymbol{V}_f^*\right] - \beta_r\left[\boldsymbol{r}(t) - \boldsymbol{r}_f^* + \boldsymbol{V}_f^* t_{go}\right]\end{aligned} \tag{13}$$

where again and henceforth the arguments of the functions have been omitted. Now let us choose β_V and β_r such that the coefficients of $\boldsymbol{c}_1$ and $\boldsymbol{c}_2$ in Eq. (13) vanish:

$$\phi_1 + \beta_V\bar{\phi}_1 + \beta_r\hat{\phi}_1 = 0 \tag{14}$$

$$\phi_2 + \beta_V\bar{\phi}_2 + \beta_r\hat{\phi}_2 = 0 \tag{15}$$

The solution is

$$\beta_r^* = \frac{-\bar{\phi}_2\phi_1 + \bar{\phi}_1\phi_2}{\Delta} \tag{16}$$

$$\beta_V^* = \frac{\hat{\phi}_2\phi_1 + \hat{\phi}_1\phi_2}{\Delta} \tag{17}$$

where Δ is already defined in Eq. (9). We now use β_r^* and β_V^* in Eqs. (16)–(17) to replace β_r and β_V in Eq. (13). The resulting guidance law is

$$\boldsymbol{a}_T = \boldsymbol{g}t_{go}\left(\frac{1}{2}\beta_r^* t_{go} - \beta_V^*\right) - \beta_V^*\left[\boldsymbol{V}(t) - \boldsymbol{V}_f^*\right] - \beta_r^*\left[\boldsymbol{r}(t) - \boldsymbol{r}_f^* + \boldsymbol{V}_f^* t_{go}\right] \tag{18}$$

It is instructive to observe a special case. If $\phi_1 = 1$ and $\phi_2 = t_{go}$, Eqs. (16) and (17) give

$$\beta_r^* = \frac{6}{t_{go}^2},\quad \beta_V^* = \frac{4}{t_{go}} \tag{19}$$

and guidance law (18) becomes (after a slight re-arrangement of terms)

$$\boldsymbol{a}_T = -\frac{2}{t_{go}}\left[\boldsymbol{V}_f^* - \boldsymbol{V}(t)\right] + \frac{6}{t_{go}^2}\left[\boldsymbol{r}_f^* - \boldsymbol{r}(t) - \boldsymbol{V}(t)t_{go}\right] - \boldsymbol{g} \tag{20}$$

This is precisely the E-guidance law in Ref. [2]! Recall that the E-guidance law is derived as an explicit guidance law. [2] But Eq. (18) comes from the implicit tracking law in Eq. (12). This observation turns out to manifest a general property as delineated in the following.

The particular set of the gain functions of β_V^* and β_r^* in Eqs. (16) and (17) null the coefficients of $\boldsymbol{c}_1$ and $\boldsymbol{c}_2$ in Eq. (13). Therefore with these two feedback gains the guidance law in Eq. (12) (equivalently Eq. (13)) are not affected by the changes in $\boldsymbol{c}_1$ and $\boldsymbol{c}_2$. However, this does not mean that $\boldsymbol{c}_1$ and $\boldsymbol{c}_2$ can be arbitrary, as the conclusion that any $\boldsymbol{c}_1$ and $\boldsymbol{c}_2$ will do obviously makes no sense, in light of their influence on the reference profiles in Eqs. (6),

(10) and (11). The correct interpretation is that $\boldsymbol{c}_1$ and $\boldsymbol{c}_2$ must be uniquely determined in this case thus no variations in $\boldsymbol{c}_1$ and $\boldsymbol{c}_2$ are allowed. The only way $\boldsymbol{c}_1$ and $\boldsymbol{c}_2$ are uniquely determined in this problem is to select them to meet the targeting condition in Eqs. (3) and (4), using the current state $\{\boldsymbol{r}(t), \boldsymbol{V}(t)\}$ as the initial condition. The following proposition formalizes this conclusion.

Proposition 1—At any given $t \le t_f$ and with given current position $\boldsymbol{r}(t)$ and velocity $\boldsymbol{V}(t)$, we solve $\boldsymbol{c}_1$ and $\boldsymbol{c}_2$ by using the thrust acceleration profile

$$\boldsymbol{a}_T = \boldsymbol{c}_1\phi_1\left(t_{go}\right) + \boldsymbol{c}_2\phi_2\left(t_{go}\right) \tag{21}$$

to integrate Eqs. (1) and (2) with the initial condition $\{\boldsymbol{r}(t), \boldsymbol{V}(t)\}$ and to meet the final condition in Eqs. (3) and (4). Substituting the resulting $\boldsymbol{c}_1$ and $\boldsymbol{c}_2$ which are dependent on $\{\boldsymbol{r}(t), \boldsymbol{V}(t)\}$ back to Eq. (21) produces an explicit guidance law. This guidance law is the same as the one in Eq. (18) which is a particular case of the implicit tracking guidance law in Eq. (12), with the gains β_r^* and β_V^* determined in Eqs. (16) and (17).

Proof: With $\boldsymbol{a}_T$ in (21), the solutions to Eqs. (1) and (2) by backward integration are

$$\boldsymbol{r}_f^* - \boldsymbol{r}(t) = -\boldsymbol{c}_1\hat{\phi}_1 - \boldsymbol{c}_2\hat{\phi}_2 + \boldsymbol{V}_f^* t_{go} - \frac{1}{2}\boldsymbol{g}t_{go}^2 \tag{22}$$

$$\boldsymbol{V}_f^* - \boldsymbol{V}(t) = -\boldsymbol{c}_1\bar{\phi}_1 - \boldsymbol{c}_2\bar{\phi}_2 + \boldsymbol{g}t_{go} \tag{23}$$

where the current state $\{\boldsymbol{r}(t), \boldsymbol{V}(t)\}$ has been used as the condition at t, and the final position and velocity at t_f have been set to satisfy the targeting condition in Eqs. (3) and (4). Solving $\boldsymbol{c}_1$ and $\boldsymbol{c}_2$ from these two equations in terms of the other quantities, we have

$$\boldsymbol{c}_1 = \frac{-\hat{\phi}_2\left(\boldsymbol{V} - \boldsymbol{V}_f^* + \boldsymbol{g}t_{go}\right) + \bar{\phi}_2\left(\boldsymbol{r} - \boldsymbol{r}_f^* + \boldsymbol{V}_f^* t_{go} - \frac{1}{2}\boldsymbol{g}t_{go}^2\right)}{\Delta} \tag{24}$$

$$\boldsymbol{c}_2 = \frac{\hat{\phi}_1\left(\boldsymbol{V} - \boldsymbol{V}_f^* + \boldsymbol{g}t_{go}\right) - \bar{\phi}_1\left(\boldsymbol{r} - \boldsymbol{r}_f^* + \boldsymbol{V}_f^* t_{go} - \frac{1}{2}\boldsymbol{g}t_{go}^2\right)}{\Delta} \tag{25}$$

where again Δ is defined in Eq. (9). Replacing $\boldsymbol{c}_1$ and $\boldsymbol{c}_2$ in Eq. (21) with Eqs. (24) and (25) will lead to an explicit guidance law, as it is equivalent to repeatedly solving $\boldsymbol{c}_1$ and $\boldsymbol{c}_2$ at each t in this way to meet the targeting condition. The result from substituting Eqs. (24) and (25) into Eq. (21) is exactly the same as Eq. (18) with β_r^* and β_V^* in Eqs. (16) and (17). The algebraic steps involved in the back substitution and collection of terms are omitted for conciseness.

Note that for $\boldsymbol{\phi}_1 = 1$ and $\boldsymbol{\phi}_2 = t_{go}$, the E-guidance law is obtained by solving $\boldsymbol{c}_1$ and $\boldsymbol{c}_2$ just as outlined in the proof. [2] In a more general context we have shown that a particular version of the implicit guidance law in Eq. (12) is the same as the explicit guidance law.

Even though Proposition 1 shows that the same explicit guidance law can be derived either way, the approach through the use of the particular set of tracking gains in Eqs. (16) and (17) in Eq. (12) is cleaner, and it plays a central role in Section III of this paper.

B. Three-Term Parameterization

Now consider the following three-term parameterization of the reference thrust acceleration $\boldsymbol{a}_d$:

$$\boldsymbol{a}_d = \boldsymbol{a}_{T_f}^* + \boldsymbol{c}_1\phi_1(t_{go}) + \boldsymbol{c}_2\phi_2(t_{go}) \tag{26}$$

where $\boldsymbol{a}_{T_f}^* \in R^3$ is a user selected constant vector that represents the desired final thrust acceleration vector, if $\phi_1(0) = 0$ and $\phi_2(0) = 0$. The choices of ϕ_1 and ϕ_2 should still satisfy the condition in Eq. (9). The corresponding position and velocity profiles are

$$\boldsymbol{r}_d(t) = \boldsymbol{r}_f^* + \boldsymbol{c}_1\hat{\phi}_1 + \boldsymbol{c}_2\hat{\phi}_2 - \boldsymbol{V}_f^* t_{go} + \frac{1}{2}\left(\boldsymbol{g} + \boldsymbol{a}_{T_f}^*\right)t_{go}^2 \tag{27}$$

$$\boldsymbol{V}_d(t) = \boldsymbol{V}_f^* + \boldsymbol{c}_1\bar{\phi}_1 + \boldsymbol{c}_2\bar{\phi}_2 - \left(\boldsymbol{g} + \boldsymbol{a}_{T_f}^*\right)t_{go} \tag{28}$$

where the targeting conditions in Eqs. (3) and (4) have been used. The tracking law in Eq. (12) in this case becomes

$$\begin{aligned}\boldsymbol{a}_T &= \boldsymbol{c}_1\left(\phi_1 + \beta_V\bar{\phi}_1 + \beta_r\hat{\phi}_1\right) + \boldsymbol{c}_2\left(\phi_2 + \beta_V\bar{\phi}_2 + \beta_r\hat{\phi}_2\right) + \boldsymbol{a}_{T_f}^* \\ &+ \left(\boldsymbol{g} + \boldsymbol{a}_{T_f}^*\right)t_{go}\left(\frac{1}{2}\beta_r t_{go} - \beta_V\right) - \beta_V\left[\boldsymbol{V}(t) - \boldsymbol{V}_f^*\right] - \beta_r\left[\boldsymbol{r}(t) - \boldsymbol{r}_f^* + \boldsymbol{V}_f^* t_{go}\right]\end{aligned} \tag{29}$$

Therefore the same β_V^* and β_r^* in Eqs. (16) and (17) make the coefficients of $\boldsymbol{c}_1$ and $\boldsymbol{c}_2$ vanish again, and the resulting guidance law is

$$\boldsymbol{a}_T = \boldsymbol{a}_{T_f}^* + \left(\boldsymbol{g} + \boldsymbol{a}_{T_f}^*\right)\left(\frac{1}{2}\beta_r^* t_{go} - \beta_V^*\right) - \beta_V^*\left[\boldsymbol{V}(t) - \boldsymbol{V}_f^*\right] - \beta_r^*\left[\boldsymbol{r}(t) - \boldsymbol{r}_f^* + \boldsymbol{V}_f^* t_{go}\right] \tag{30}$$

Proposition 1 remains valid in this case. That is, guidance law (30) is the same as the explicit guidance law obtained by using $\boldsymbol{a}_T = \boldsymbol{a}_{T_f}^* + \boldsymbol{c}_1\phi_1(t_{go}) + \boldsymbol{c}_2\phi_2(t_{go})$ and solving $\boldsymbol{c}_1$ and $\boldsymbol{c}_2$ with the current and targeting conditions, which in this case gives

$$\boldsymbol{c}_1 = \frac{-\hat{\phi}_2\left[\boldsymbol{V} - \boldsymbol{V}_f^* + \left(\boldsymbol{g} + \boldsymbol{a}_{T_f}^*\right)t_{go}\right] + \bar{\phi}_2\left[\boldsymbol{r} - \boldsymbol{r}_f^* + \boldsymbol{V}_f^* t_{go} - \frac{1}{2}\left(\boldsymbol{g} + \boldsymbol{a}_{T_f}^*\right)t_{go}^2\right]}{\Delta} \tag{31}$$

$$\boldsymbol{c}_2 = \frac{\hat{\phi}_1\left[\boldsymbol{V} - \boldsymbol{V}_f^* + \left(\boldsymbol{g} + \boldsymbol{a}_{T_f}^*\right)t_{go}\right] - \bar{\phi}_1\left[\boldsymbol{r} - \boldsymbol{r}_f^* + \boldsymbol{V}_f^* t_{go} - \frac{1}{2}\left(\boldsymbol{g} + \boldsymbol{a}_{T_f}^*\right)t_{go}^2\right]}{\Delta} \tag{32}$$

When $\phi_1 = t_{go}$ and $\phi_2 = t_{go}^2$, the β_r^* and β_V^* by Eqs. (16) and (17) are

$$\beta_r^* = \frac{12}{t_{go}^2}, \quad \beta_V^* = \frac{6}{t_{go}} \tag{33}$$

and the guidance law in Eq. (30) becomes

$$\boldsymbol{a}_T = \boldsymbol{a}_{T_f}^* - \frac{6}{t_{go}}\left[\boldsymbol{V}_f^* - \boldsymbol{V}(t)\right] + \frac{12}{t_{go}^2}\left[\boldsymbol{r}_f^* - \boldsymbol{r}(t) - \boldsymbol{V}(t)t_{go}\right] \tag{34}$$

This is exactly the Apollo lunar descent guidance law in Refs. [3, 4] where it was originally derived to meet the targeting condition by solving $\boldsymbol{c}_1$ and $\boldsymbol{c}_2$. Here we also have shown that when the same guidance law was recovered from the tracking law (12) with the gains in Eq. (33) in Ref. [3], it was not coincidental, but just a specialization of the more general property affirmed by Proposition 1.

III. Fractional-Polynomial Guidance

A. Fractional Polynomials

Consider the following nonlinear function of a scalar variable $x \geq 0$

$$p(x) = a_0 + a_1 x^{\gamma_1} + \cdots + a_k x^{\gamma_k}, x \geq 0 \tag{35}$$

where a_i, $i = 0, 1, \ldots, k$, are real constants. The exponents γ_i's are only required to be non-negative but not necessarily integers. We shall call such a function a *fractional polynomial*. It should be recognized that $p(x)$ is not really a polynomial by the standard definition and it does not observe some of the properties of polynomials, such as that on the roots. However those properties are not needed for our purpose here. The term "fractional polynomials" has been used in statistical regression analysis [5,6] to call a function similar to $p(x)$ in Eq. (35) but whose non-integer exponents are limited to −0.5 and 0.5. Our definition here allows the exponents to be any non-negative real numbers. The inclusion of arbitrary positive exponents in the definition is essential in this paper as will become clear in Section III-C.

In the rest of this section the basis functions ϕ_1 and ϕ_2 in Section II will be chosen to be fractional polynomials. Everything developed in Section II for general ϕ_1 and ϕ_2 not only remains applicable to fractional polynomials, but in many cases yields simple and clean results with fractional polynomials.

B. Fractional-Polynomial Guidance Laws

We will specialize the parameterization in Eq. (6) by a fractional polynomial of t_{go}

$$\boldsymbol{a}_d = \boldsymbol{c}_1 + \boldsymbol{c}_2 t_{go}^{\gamma}, \quad \gamma > 0 \tag{36}$$

where $\gamma > 0$ is a constant, and the coefficient vectors $\boldsymbol{c}_1$ and $\boldsymbol{c}_2$ are to be determined. Let $\boldsymbol{c}_1 = \boldsymbol{a}_{T_f}^*$, the desired final thrust acceleration vector. Thus

$$\boldsymbol{a}_d = \boldsymbol{a}_{T_f}^* + \boldsymbol{c}_2 t_{go}^{\gamma}, \quad \gamma > 0 \tag{37}$$

Clearly in this instance

$$\phi_1 = 1, \bar{\phi}_1 = -t_{go}, \hat{\phi}_1 = \frac{1}{2} t_{go}^2 \tag{38}$$

$$\phi_2 = t_{go}^{\gamma}, \bar{\phi}_2 = -\frac{1}{\gamma+1} t_{go}^{\gamma+1}, \hat{\phi}_2 = \frac{1}{(\gamma+1)(\gamma+2)} t_{go}^{\gamma+2} \tag{39}$$

The reference position and velocity profiles $\boldsymbol{r}_d$ and $\boldsymbol{V}_d$ with the above functions are readily constructed by Eqs. (10) and (11), and the tracking law formed according to Eq. (13). By Eqs. (16) and (17) we have the particular set of the gain functions in this case as

$$\beta_r^* = \frac{2(\gamma+2)}{t_{go}^2}, \quad \beta_V^* = \frac{\gamma+3}{t_{go}} \tag{40}$$

These two expressions prompt us to choose in general the feedback gain functions β_r and β_V to be

$$\beta_r = \frac{k_r}{t_{go}^2}, \quad \beta_V = \frac{k_V}{t_{go}} \tag{41}$$

where k_r and k_V are constants. To avoid the need to have to decide on what $\boldsymbol{c}_2$ should be in the parameterization in Eq. (37), we will choose k_r and k_V by Eq. (15) to eliminate the coefficient of the to-be-determined vector $\boldsymbol{c}_2$. With the β_r and β_V in Eq. (41) and the functions in Eq. (39), Eq. (15) in this case leads to

$$k_V = \frac{1}{\gamma+2} k_r + \gamma + 1 \tag{42}$$

The guidance law in Eq. (13) then is independent of $\boldsymbol{c}_2$, and for obvious reason we shall call the result in this case the fractional-polynomial powered descent guidance (FP^{2}DG) law

$$\begin{aligned} \boldsymbol{a}_T = {} & \gamma\left[\frac{k_r}{2(\gamma+2)} - 1\right]\boldsymbol{a}_{T_f}^* + \left[\frac{\gamma k_r}{2(\gamma+2)} - \gamma - 1\right]\boldsymbol{g} + \frac{(\gamma+1)}{t_{go}}\left(1 - \frac{k_r}{\gamma+2}\right)\left(\boldsymbol{V}_f^* - \boldsymbol{V}\right) \\ & + \frac{k_r}{t_{go}^2}\left(\boldsymbol{r}_f^* - \boldsymbol{r} - \boldsymbol{V} t_{go}\right) \end{aligned} \tag{43}$$

This is a guidance law with a gain parameter k_r and another parameter γ that can both be adjusted. It should be stressed that despite of the fractional exponent γ in the parameterization (37), no terms involving fractional exponents are present in the guidance law (43). An elegant interpretation to this guidance law for an arbitrary k_r will be given in the next subsection. For now, reminded by Eq. (40), if we choose

$$k_r = 2(\gamma + 2) \tag{44}$$

which gives $k_V = \gamma + 3$ by Eq. (42), the guidance law (43) reduces to

$$\boldsymbol{a}_T = -\boldsymbol{g} - \frac{(\gamma+1)}{t_{go}}\left(\boldsymbol{V}_f^* - \boldsymbol{V}\right) + \frac{2(\gamma+2)}{t_{go}^2}\left(\boldsymbol{r}_f^* - \boldsymbol{r} - \boldsymbol{V}t_{go}\right) \tag{45}$$

According to the Proposition 1 and the discussion in Section II-A, this is the same as the explicit guidance law obtained by directly solving $\boldsymbol{c}_1$ and $\boldsymbol{c}_2$ in Eq. (36) to meet the targeting condition.

A particularly important version of the FP^{2}DG law (43) is when $\gamma = 1$:

$$\boldsymbol{a}_T = \left(\frac{k_r}{6} - 1\right)\boldsymbol{a}_{T_f}^* + \left(\frac{k_r}{6} - 2\right)\boldsymbol{g} + \frac{2}{t_{go}}\left(1 - \frac{k_r}{3}\right)\left(\boldsymbol{V}_f^* - \boldsymbol{V}\right) + \frac{k_r}{t_{go}^2}\left(\boldsymbol{r}_f^* - \boldsymbol{r} - \boldsymbol{V}t_{go}\right) \tag{46}$$

This is the augmented Apollo powered descent guidance (A^{2}PDG) law developed in Ref. [1]. When $k_r = 2(\gamma + 2) = 6$, the above guidance law is the famous E-guidance law (the same as Eq. (45) with $\gamma = 1$). It is also discovered in Ref. [1] that, with $k_r = 12$, the A^{2}PDG law becomes the Apollo lunar descent guidance law (cf. Eq. (34)). These discoveries were surprising, especially the latter because the Apollo lunar descent guidance law is the result of using a quadratic thrust acceleration. [3, 4] But the author was unable to identify the underlying reasons then. Proposition 1 in this paper answers the first part of the puzzle (on why the A^{2}PDG law becomes E-guidance). The reason for the second part will be revealed in the next subsection.

C. Equivalence in Fractional-Polynomial Guidance

As far as we understand up to this point, other than the way in which k_V is specified by Eq. (42), the FP^{2}DG law in Eq. (43) originates from and should remain a tracking law from the general form Eq. (12). One would expect that the response of a typical tracking control law and the closeness of achieving the specified targeting condition, a measure of the tracking performance, would be strongly dependent on its gains. This expectation does not reconcile well at all with the observation that for all values of k_r above a threshold value (which will be identified in this subsection), the FP^{2}DG law in Eq. (43) performs in a very predicable way and its targeting accuracy is always very good. And the fact cannot be just a coincidence that two different values of k_r in the A^{2}PDG law [1] (which is Eq. (43) with γ = 1) produce respectively the E-guidance law and Apollo lunar descent guidance law both of which are explicit guidance laws, but one is based on a linear thrust acceleration and the other quadratic. All these peculiarities seem to suggest something deeper, but the answer has remained elusive, until now.

Now we are ready to offer the answers. To this end we will need to first develop the explicit guidance law based on the following fractional polynomial parameterization of thrust acceleration in the form of Eq. (26)

$$\boldsymbol{a}_d = \boldsymbol{a}_{T_f}^* + \boldsymbol{c}_1 t_{go}^{\gamma_1} + \boldsymbol{c}_2 t_{go}^{\gamma_2}, \ \ \gamma_1 \ge 0, \gamma_2 \ge 0 \tag{47}$$

where γ_1 and γ_2 are two positive real numbers. The associated functions for the two basis functions are then

$$\phi_i = t_{go}^{\gamma_i}, \bar{\phi}_i = -\frac{1}{\gamma_i + 1} t_{go}^{\gamma_i + 1}, \hat{\phi}_i = \frac{1}{(\gamma_i + 1)(\gamma_i + 2)} t_{go}^{\gamma_i + 2}, \ \ i = 1, 2 \tag{48}$$

Following the discussion in Section II-B and applying Eqs. (16) and (17) to obtain the particular set of the feedback gains in the tracking law (12), we arrive at

$$\beta_r^* = \frac{(\gamma_1 + 2)(\gamma_2 + 2)}{t_{go}^2}, \ \ \beta_V^* = \frac{\gamma_1 + \gamma_2 + 3}{t_{go}} \tag{49}$$

With these gains, the guidance law in Eq. (30) takes the form of

$$\begin{aligned} \boldsymbol{a}_T = \boldsymbol{a}_{T_f}^* &+ \left(\frac{1}{2}\gamma_1\gamma_2 - 1\right)\left(\boldsymbol{a}_{T_f}^* + \boldsymbol{g}\right) - \frac{1}{t_{go}}(\gamma_1\gamma_2 + \gamma_1 + \gamma_2 + 1)\left(\boldsymbol{V}_f^* - \boldsymbol{V}\right) \\ &+ \frac{(\gamma_1 + 2)(\gamma_2 + 2)}{t_{go}^2}\left(\boldsymbol{r}_f^* - \boldsymbol{r} - \boldsymbol{V} t_{go}\right) \end{aligned} \tag{50}$$

It is interesting to note that everything so far in this subsection remains valid even if $\gamma_1 = \gamma_2$, in which case the assumption in Eq. (9) does not hold. By Proposition 1, guidance law (50) is the same as the explicit guidance law from the fractional-polynomial thrust acceleration profile:

$$\boldsymbol{a}_T = \boldsymbol{a}_{T_f}^* + \boldsymbol{c}_1 t_{go}^{\gamma_1} + \boldsymbol{c}_2 t_{go}^{\gamma_2}, \ \ \gamma_1 \ge 0, \gamma_2 \ge 0 \tag{51}$$

The following proposition connects the FP^{2}DG law in Eq. (43) to guidance law (50).

Proposition 2—For any $\gamma > 0$ and $k_r \ge 2(\gamma + 2)$, the FP^{2}DG law in Eq. (43) is equivalent to another fractional-polynomial *explicit* powered descent guidance law of the form in Eq. (50) with the values of γ_1 and γ_2 given as follows

$$\gamma_{1,2} = \begin{cases} \gamma, \\ \dfrac{k_r}{\gamma + 2} - 2 \end{cases} \tag{52}$$

Proof: Re-arrange Eq. (43) slightly to be consistent with the format of Eq. (50)

$$\boldsymbol{a}_T = \boldsymbol{a}^*_{T_f} + \left[\frac{\gamma k_r}{2(\gamma+2)} - \gamma - 1\right]\left(\boldsymbol{a}^*_{T_f} + \boldsymbol{g}\right) + \frac{(\gamma+1)}{t_{go}}\left(1 - \frac{k_r}{\gamma+2}\right)\left(\boldsymbol{V}^*_f - \boldsymbol{V}\right) + \frac{k_r}{t_{go}^2}\left(\boldsymbol{r}^*_f - \boldsymbol{r} - \boldsymbol{V}t_{go}\right) \tag{53}$$

Comparing the coefficients of the like terms in Eqs. (50) and (53), we require the following 3 equations for the two guidance laws to be equivalent to each other

$$\frac{1}{2}\gamma_1\gamma_2 - 1 = \frac{\gamma k_r}{2(\gamma+2)} - \gamma - 1 \tag{54}$$

$$-\left(\gamma_1\gamma_2 + \gamma_1 + \gamma_2 + 1\right) = (\gamma+1)\left(1 - \frac{k_r}{\gamma+2}\right) \tag{55}$$

$$\left(\gamma_1 + 2\right)\left(\gamma_2 + 2\right) = k_r \tag{56}$$

Upon a closer inspection, it is realized that these three equations are not linearly independent, but only two of them are. Hence we can use any two equations to solve γ_1 and γ_2 in terms of γ and k_r. The unique solution is found to be the one in Eq. (52), and it satisfies all the 3 conditions in Eqs. (54)–(56).

Discussion:

1. Proposition 2 provides a simple explanation to the good performance of the FP^{2}DG law (43): It turns out that for any given $\gamma > 0$ and $k_r > 2(\gamma + 2)$, the tracking law in Eq. (43) is actually the explicit guidance law based on the thrust acceleration profile in Eq. (51). Or to put it in another way: for every $\gamma > 0$, by simply changing the gain k_r in Eq. (43), we will have a family of explicit guidance laws, each explicitly commanding a (different) trajectory from the same current state to the same specified targeting condition at t_f.

2. Again the case of $\gamma = 1$ is of particular interest because of its connection to Apollo powered descent guidance designs. And Proposition 2 solves the puzzle why the A^{2}PDG law in Ref. [1] becomes the E-guidance law when $k_r = 6$ and Apollo lunar descent guidance law when $k_r = 12$. This is because the A^{2}PDG law is Eq. (43) with $\gamma = 1$; when $k_r = 6$, Eq. (52) gives $\gamma_1 = 1$ and $\gamma_2 = 0$, and Eq. (51) reduces to

$$\boldsymbol{a}_T = \boldsymbol{c}_0 + \boldsymbol{c}_1 t_{go}$$

where $\boldsymbol{c}_0 = \boldsymbol{a}^*_{T_f} + \boldsymbol{c}_2$. By Proposition 2 the A^{2}PDG is the explicit guidance law based on this linear thrust acceleration profile, which is precisely how the E-guidance law comes about. On the other hand, when $k_r = 12$, Eq. (52) gives $\gamma_1 =$

1 and $\gamma_2 = 2$. Hence the A[2]PDG law, by Proposition 2, is the explicit guidance law based on the thrust acceleration profile

$$\boldsymbol{a}_T = \boldsymbol{a}^*_{T_f} + \boldsymbol{c}_1 t_{go} + \boldsymbol{c}_2 \tau^2_{go}$$

This is exactly how the Apollo lunar descent guidance law is derived.

3. Another point that highlights the power of the implicit-to-explicit guidance development approach in this paper is the case of $k_r = (\gamma + 2)^2$ – for instance, $k_r = 9$ when $\gamma = 1$. This k_r is greater than $2(\gamma + 2)$ as required for any $\gamma > 0$. For $k_r = (\gamma + 2)^2$ the guidance law in Eq. (43) is well defined, and $\gamma_1 = \gamma_2 = \gamma$ by Eq. (52). Proposition 2 remains applicable, that is, the guidance law in Eq. (43) is an explicit guidance law that targets the terminal constraints in Eqs. (3) and (4). However, if in this case one were to attempt to derive the explicit guidance law directly by solving $\boldsymbol{c}_1$ and $\boldsymbol{c}_2$ in Eq. (51), a difficulty would arise because the denominator $\Delta = 0$ in the solutions of $\boldsymbol{c}_1$ and $\boldsymbol{c}_2$ as given in Eqs. (24) and (25), due to the fact that $\gamma_1 = \gamma_2$.

IV. Automated Beyond-Termination Targeting

Proposition 2 establishes that $\boldsymbol{r} \to \boldsymbol{r}^*_f$ and $\boldsymbol{V} \to \boldsymbol{V}^*_f$ as $t_{go} \to 0$ for any $\gamma > 0$ and $k_r \geq 2(\gamma + 2)$. Therefore the two vanishing denominators in the expression of $\boldsymbol{a}_T$ in Eq. (43) at $t_{go} = 0$ do not necessarily indicate a theoretical singularity. Indeed, by applying the L'Hospital's rule, we can readily show that

$$\lim_{t_{go} \to 0} \left(\frac{\boldsymbol{V}^*_f - \boldsymbol{V}}{t_{go}} \right) = \boldsymbol{a}_T\left(t_f\right) + \boldsymbol{g} \tag{57}$$

$$\lim_{t_{go} \to 0} \left(\frac{\boldsymbol{r}^*_f - \boldsymbol{r} - \boldsymbol{V} t_{go}}{t^2_{go}} \right) = \frac{1}{2}\left[\boldsymbol{a}_T\left(t_f\right) + \boldsymbol{g}\right] \tag{58}$$

Using these two equations in the guidance law in Eq. (43) and arranging terms strategically, we have

$$\boldsymbol{a}_T\left(t_f\right)\left[\frac{k_r}{2(\gamma + 2)} - 1\right]\gamma = \boldsymbol{a}^*_{T_f}\left[\frac{k_r}{2(\gamma + 2)} - 1\right]\gamma \tag{59}$$

When $k_r > 2(\gamma + 2)$ (and since $\gamma > 0$), it follows that

$$\boldsymbol{a}_T\left(t_f\right) = \boldsymbol{a}^*_{T_f} \tag{60}$$

When $k_r = 2(\gamma + 2)$, $\boldsymbol{a}_T(t_f)$ remains finite as Eqs. (57) and (58) are still valid. In this case since $\boldsymbol{a}^*_{T_f}$ vanishes from the guidance law in Eq. (43), $\boldsymbol{a}_T(t)$, including $\boldsymbol{a}_T(t_f)$, is independent of $\boldsymbol{a}^*_{T_f}$. However, Eq. (59) is unable to identify uniquely $\boldsymbol{a}_T(t_f)$ for the case where $k_r = 2(\gamma + 2)$.

The above development actually corrects a discussion on the theoretical value of $\boldsymbol{a}_T(t_f)$ in Ref. [1] for the A^{2}PDG law, and shows that the final commanded thrust acceleration vector with any $k_r > 2(\gamma + 2)$ is always $\boldsymbol{a}^*_{T_f}$ for the FP^{2}DG family of which A^{2}PDG law is a part.

In actual flight, navigation uncertainty and the effects of the rotational dynamics and control system not modeled in the guidance solution will cause the errors in meeting precisely the targeting condition $\boldsymbol{r}\left(t_f\right) = \boldsymbol{r}^*_f$ and $\boldsymbol{V}\left(t_f\right) = \boldsymbol{V}^*_f$. Therefore a practical singularity in Eq. (43) can be present at $t_{go} = 0$, and the guidance command may start to diverge as $t_{go} \to 0$ if $\boldsymbol{r}(t)$ does not approach sufficiently close to $\boldsymbol{r}^*_f$ and $\boldsymbol{V}(t)$ to $\boldsymbol{V}^*_f$. In the Apollo lunar descent guidance, the targeting condition and t_{go} are said to be actually chosen beyond the intended guidance termination point to avoid the singularity, [3, 4] although no specifics on how are reported. Here a similar idea is adopted, but the technique is formalized for FP^{2}DG, with detailed functional relationship between the targeting condition beyond the intended guidance termination and the desired condition at the guidance termination. More importantly, this targeting is automated to use the current trajectory state and embedded as a part of the closed-loop guidance solution in a guidance cycle, to ensure the accurate attainment of the required condition at the termination of guidance, even with substantial trajectory dispersion.

The idea of beyond-termination targeting is illustrated in Fig. 1. The FP^{2}DG law is targeting a point beyond the actual guidance termination with the to-be-determined final condition defined by the triplet $(\boldsymbol{r}_f, \boldsymbol{V}_f, \boldsymbol{a}_{T_f})$ and a given time-to-go t_{go}. For a prescribed constant $\Delta t_{go} > 0$ (and $\Delta t_{go} < t_{go}$), the targeting condition $(\boldsymbol{r}_f, \boldsymbol{V}_f, \boldsymbol{a}_{T_f})$ is chosen such at the trajectory passes the required targeting condition $(\boldsymbol{r}^*_f, \boldsymbol{V}^*_f, \boldsymbol{a}^*_{T_f})$ at $t_{go} = \Delta t_{go}$ where the actual guidance terminates. Hence the true time-to-go for the guidance is $t^*_{go} = t_{go} - \Delta t_{go}$.

Proposition 2 enables us to obtain analytically the explicit solutions of $(\boldsymbol{r}(t), \boldsymbol{V}(t), \boldsymbol{a}_T(t))$ as functions of time when $\boldsymbol{a}_T$ is given by the FP^{2}DG law in Eq. (43). This in turn allows the establishment of the linear equations that relate $(\boldsymbol{r}_f, \boldsymbol{V}_f, \boldsymbol{a}_{T_f})$ to $(\boldsymbol{r}^*_f, \boldsymbol{V}^*_f, \boldsymbol{a}^*_{T_f})$ for given t_{go}, Δt_{go}, and current state $(\boldsymbol{r}(t), \boldsymbol{V}(t))$:

$$\begin{bmatrix} \boldsymbol{r}_f \\ \boldsymbol{V}_f \\ \boldsymbol{a}_{T_f} \end{bmatrix} = M^{-1}\left\{\begin{bmatrix} \boldsymbol{r}^*_f \\ \boldsymbol{V}^*_f \\ \boldsymbol{a}^*_{T_f} \end{bmatrix} - \boldsymbol{b}\left(\boldsymbol{r}(t), \boldsymbol{V}(t), t_{go}, \Delta t_{go}\right)\right\} \tag{61}$$

where $M \in R^{9\times 9}$ depends on t_{go} and Δt_{go}, and $\boldsymbol{b} \in R^9$ is a function of $\boldsymbol{r}(t)$, $\boldsymbol{V}(t)$, t_{go}, and Δt_{go}. The detailed functional expressions and more in-depth elaboration are given in the

Appendix. The current t_{go} and the obtained triplet $(\boldsymbol{r}_f, \boldsymbol{V}_f, \boldsymbol{a}_{T_f})$ are used in the guidance law in Eq. (43) in place of $(\boldsymbol{r}_f^*, \boldsymbol{V}_f^*, \boldsymbol{a}_{T_f}^*)$. The current powered descent flight phase terminates at $t_{go} = \Delta t_{go} > 0$ where the trajectory will achieve the condition $(\boldsymbol{r}_f^*, \boldsymbol{V}_f^*, \boldsymbol{a}_{T_f}^*)$. To adapt to trajectory dispersions, Eq. (61) is used in each guidance cycle with the current state $(\boldsymbol{r}(t), \boldsymbol{V}(t))$ to update the targeting condition $(\boldsymbol{r}_f, \boldsymbol{V}_f, \boldsymbol{a}_{T_f})$ to ensure that $(\boldsymbol{r}_f^*, \boldsymbol{V}_f^*, \boldsymbol{a}_{T_f}^*)$ is closely achieved at $t_{go} = \Delta t_{go}$.

This beyond-termination targeting method is very insensitive to the value of Δt_{go}, with nearly the same guidance performance for a Δt_{go} of several seconds to tens of seconds.

V. Recapitulation and Numerical Illustrations

A. Recapitulation

For the benefit of the reader, a succinct summary is given below to recap the more important or interesting findings so far.

1. By using the reference thrust acceleration profile $\boldsymbol{a}_d = \boldsymbol{a}_{T_f}^* + \boldsymbol{c}_2 t_{go}^{\gamma}$ and the corresponding radius and velocity profiles $\boldsymbol{r}_d$ and $\boldsymbol{V}_d$ in the tracking law

$$\boldsymbol{a}_T = \boldsymbol{a}_d - \frac{k_V}{t_{go}}(\boldsymbol{V} - \boldsymbol{V}_d) - \frac{k_r}{t_{go}^2}(\boldsymbol{r} - \boldsymbol{r}_d)$$

and choosing k_V to eliminate $\boldsymbol{c}_2$ from $\boldsymbol{a}_T$, we arrive at the FP^{2}DG law in Eq. (43), reproduced in the following

$$\boldsymbol{a}_T = \gamma\left[\frac{k_r}{2(\gamma+2)} - 1\right]\boldsymbol{a}_{T_f}^* + \left[\frac{\gamma k_r}{2(\gamma+2)} - \gamma - 1\right]\boldsymbol{g} + \frac{(\gamma+1)}{t_{go}}\left(1 - \frac{k_r}{\gamma+2}\right)\left(\boldsymbol{V}_f^* - \boldsymbol{V}\right) + \frac{k_r}{t_{go}^2}\left(\boldsymbol{r}_f^* - \boldsymbol{r} - \boldsymbol{V}t_{go}\right) \tag{62}$$

This equation represents a family of two-parameter guidance laws for all $\gamma > 0$ and $k_r \geq 2(\gamma + 2)$. For any such pair of $\{\gamma, k_r\}$, each member of this family of guidance laws is the same as the explicit guidance law corresponding to the thrust acceleration profile parameterized by

$$\boldsymbol{a}_T = \boldsymbol{a}_{T_f}^* + \boldsymbol{c}_1 t_{go}^{\gamma_1} + \boldsymbol{c}_2 t_{go}^{\gamma_2}, \quad \gamma_1 = \gamma, \gamma_2 = \frac{k_r}{\gamma+2} - 2 \tag{63}$$

This explicit guidance law can be obtained by solving the coefficients $\boldsymbol{c}_1$ and $\boldsymbol{c}_2$ using the current state as the initial condition and the targeting condition in Eqs. (3) and (4) as the final condition. The resulting guidance law is identical to Eq. (62).

2. An important subset of the FP^{2}DG law family of Eq. (62) is when $\gamma = 1$ and for any $k_r \geq 6$, i. e., Eq. (62) specializes to be the A^{2}PDG law in Ref. [1]

$$\boldsymbol{a}_T = \left(\frac{k_r}{6} - 1\right)\boldsymbol{a}^*_{T_f} + \left(\frac{k_r}{6} - 2\right)\boldsymbol{g} + \frac{2}{t_{go}}\left(1 - \frac{k_r}{3}\right)\left(\boldsymbol{V}^*_f - \boldsymbol{V}\right) + \frac{k_r}{t^2_{go}}\left(\boldsymbol{r}^*_f - \boldsymbol{r} - \boldsymbol{V}t_{go}\right) \tag{64}$$

In this case the FP^{2}DG laws are the same as the explicit guidance laws based on the thrust acceleration profile (cf. Proposition 2)

$$\boldsymbol{a}_T = \boldsymbol{a}^*_{T_f} + \boldsymbol{c}_1 t_{go} + \boldsymbol{c}_2 t_{go}^{\left(k_r/3 - 2\right)} \tag{65}$$

This family includes the E-guidance law when $k_r = 6$ and Apollo lunar descent guidance law when $k_r = 12$, for any $\boldsymbol{a}^*_{T_f}$.

3. It is interesting to note that for $\gamma = 2$, the value of $k_r = 12$ also leads Eq. (62) to produce the Apollo lunar descent guidance for any $\boldsymbol{a}^*_{T_f}$. But the E-guidance law will not be realized for any k_r in this case.

4. When k_r is held at $2(\gamma + 2)$, and γ is allowed to take any positive value, the FP^{2}DG law, now in the form of

$$\boldsymbol{a}_T = -\boldsymbol{g} - \frac{(\gamma + 1)}{t_{go}}\left(\boldsymbol{V}^*_f - \boldsymbol{V}\right) + \frac{2(\gamma + 2)}{t^2_{go}}\left(\boldsymbol{r}^*_f - \boldsymbol{r} - \boldsymbol{V}t_{go}\right) \tag{66}$$

is the explicit guidance law based on the thrust acceleration profile

$$\boldsymbol{a}_T = \boldsymbol{c}_1 + \boldsymbol{c}_2 t^\gamma_{go}, \quad \gamma > 0 \tag{67}$$

B. Numerical Illustrations

For numerical demonstration, a heavy-mass entry, descent and landing mission scenario at Mars is used. The vehicle is a mid lift-to-drag ratio rigid vehicle designed for a human Mars mission. [7] At the entry interface the vehicle has a mass of 62 metric tons. Entry flight starts at an initial downrange of about 1200 km, and the entry trajectory is guided by a predictor-corrector entry guidance algorithm. [8] A supersonic retropropulsion system with a total maximum vacuum thrust of 800,000 Newtons is employed for powered descent and landing. The thrust vector is in the body-normal direction. The vehicle touches down horizontally. Figure 2 shows a snapshot of an animation of the vehicle during powered descent. See Ref. [1] for additional detail about the vehicle and mission. For the illustrations in this section the powered descent initiation (PDI) where the engine ignites is at a ground range of 20 km to the landing site. All powered descent trajectories shown in this section have the same PDI condition and touchdown condition, as well as the same initial t_{go} of 100 seconds. A choice of $\boldsymbol{a}^*_{T_f} = -2\boldsymbol{g}$ (where $\boldsymbol{g}$ is the gravitational acceleration at the surface of Mars) is used in all guidance laws wherever $\boldsymbol{a}^*_{T_f}$ is needed, unless stated otherwise. The numerical illustrations are generated by three-degree-of-freedom closed-loop simulations where the guidance law is called at a rate of 10 Hz.

1. Testing Fractional-Polynomial Guidance

Effects of k_r: First the FP²DG law (62) is demonstrated with $\gamma = 1$ and several values of k_r. Figure 3 shows the altitude versus ground range along the powered descent trajectories (again recall that $k_r = 6$ gives the E-guidance law and $k_r = 12$ leads to the Apollo lunar descent guidance law). While the influence of the variation of k_r in shaping the trajectory is clear and strong, the trajectories are all well behaved in a very predicable fashion as k_r varies. This predictability is explained by Proposition 2 in that for each k_r the guidance law (62) is the explicit guidance law from the thrust acceleration parameterization (65), and the trajectory should exhibit a gradual behavior as k_r varies continuously. The variations of altitude versus velocity are depicted in Fig. 4. The powered descent trajectories with a smaller k_r have higher velocity at the same altitude, sometimes twice of the velocity on the trajectory with $k_r = 15$. The engine throttle settings along the trajectories are plotted in Fig. 5. While not shown in a figure, the angle between the thrust and velocity vectors is typically in the neighborhood of 180 deg most of the time (although not exactly a gravity turn). Thus the throttle changes are reflecting the fact that the guidance law uses the thrust modulation mainly to control the velocity magnitude.

If no gimbaling of the engine nozzle is considered, the direction of $\boldsymbol{a}_T$ defines the required body attitude of the vehicle, and the body Euler angles can be determined. The vehicle body Euler angles in a 3-2-1 rotation sequence with respect to the North-East-Down coordinate frame at the landing site are calculated this way. The pitch angle profiles are given in Fig. 6. They do have some considerable variations, as expected by the different trajectory shapes in Fig. 3. Note that a final pitch angle of zero means a horizontal touchdown for the vehicle model used.

For the fixed $\gamma = 1$, propellant consumption generally increases with k_r. When $k_r = 6$ (E-guidance), the solution is actually optimal in the sense of minimizing a quadratic performance index of the thrust acceleration. [9] But the difference in propellant consumption between the case of $k_r = 6$ and case of $k_r = 15$ is only 350 kg, about 0.7% of the touchdown mass of the vehicle.

Effects of γ: To see the influence of the variations of γ, we use a fixed $k_r = 15$ in Eq. (62), but vary the values of γ. Figure 7 illustrates the trajectories for 4 different values of γ. Note that for $k_r = 15$, it can be easily verified that $\gamma = 2$ and $\gamma = 3$ give the identical guidance law from Eq. (62). The throttle settings are plotted in Fig. 8. The influence of γ is not as monotonic as that of k_r, but the trajectories are still well behaved. The propellant usage is also not monotonic, and the trajectory with $\gamma = 5$ has the least propellant usage of 11394 kg. This trajectory (with $\gamma = 5$) is actually quite close to that under the E-guidance law (with $\gamma = 1$ and $k_r = 6$) which incurs a propellant usage of 11434 kg. The fact that the propellant usage under the guidance law (62) with $\gamma = 5$ and $k_r = 15$ is (slightly) better than that of the E-guidance law is not an error: the E-guidance is optimal in minimizing the quadratic performance index $J = \int_{t_0}^{t_f} \|\boldsymbol{a}_T\|^2 dt$, whereas the minimum propellant consumption requires a performance index such as $J = \int_{t_0}^{t_f} \|\boldsymbol{a}_T\| dt$.

2. Comparison with Tracking Guidance—As a comparison to the FP^{2}DG laws, we next use the basis functions in Eqs. (38) and (39) with $\gamma = 1$, and Eq. (41) in the tracking law (12) to compute the guidance command from

$$\boldsymbol{a}_T = \boldsymbol{a}_d - \frac{k_V}{t_{go}}\left[\boldsymbol{V}(t) - \boldsymbol{V}_d(t)\right] - \frac{k_r}{t_{go}^2}\left[\boldsymbol{r}(t) - \boldsymbol{r}_d(t)\right] \tag{68}$$

A generic tracking law (thus implicit guidance) sets the values k_r and k_V independently, that is, they do not need to satisfy Eq. (42). Several pairs of values for the two gains k_r and k_V are used for testing and the trajectories are shown in Fig. 9. Unlike the orderly pattern seen in Fig. 3, the trajectories now behave sporadically and in some cases drastically as k_r and k_V vary. The trajectories in solid red and black in Fig. 9 are the same as those in Fig. 3 but they no longer form the envelope of the trajectories as in Fig. 3. It is worth noting that for some values of k_r and k_V the trajectory would fail to achieve the specified targeting condition because of engine thrust saturation at the maximum, for instance $k_r = 8$ and $k_V = 5$, even though this is a pair close to several pairs of the values in Fig. 9 that do work. Figure 10 illustrates the variations of the engine throttle settings. They are volatile and could pose problems for engine throttling control. Not surprisingly the two most benign throttle profiles are those with $k_r = 6$ and $k_V = 4$ (E-guidance) and $k_r = 15$ and $k_V = 7$, two members of the tunable guidance laws in Eq. (62). The pitch angle profiles are in Fig. 14. Again in some cases (e.g., for $k_r = 12$ and $k_V = 5$) the variations may be too much and cause potential stability and control concerns.

This comparison between the fractional-polynomial guidance (62) and generic tracking guidance (68) offers compelling evidence to the superiority of the FP^{2}DG approach.

3. Effects of Fractional Exponents—Lastly we take a look at the guidance law in Eq. (66) for various values of γ. Recall that Eq. (66) is the case of Eq. (62) when $k_r = 2(\gamma + 2)$, and is the explicit guidance law based on

$$\boldsymbol{a}_T = \boldsymbol{c}_1 + \boldsymbol{c}_2 t_{go}^{\gamma}$$

Figure. 12 shows the final portions of the trajectories. The differences on a larger scale are quite minor as γ is increased from 0.7 to 3.0. The differences in propellant consumption are practically negligible, with the largest differential at 54 kg (about 0.1% of the total landing mass). The throttle settings are all relatively close as seen in Fig. 13. Notice that all the throttle settings are monotonically decreasing. This is a thrust property required in the Apollo powered descent design. [10] The pitch angles in Fig. 14 however do indicate a difference at touchdown: the smaller γ is, the smaller a final pitch angle will be at touchdown (closer to horizontal landing for the vehicle model used). In general this testing suggests that when k_r is set at $2(\gamma + 1)$ the variation of γ has a weaker influence on the guidance and trajectory as compared to Figs. 7–8 where γ is varied but k_r is fixed at a constant value independent of γ.

The numerical results in this section are intended only for the demonstration of some of the salient features of the FP^{2}DG law. The performance of the A^{2}PDG law (an important member of the FP^{2}DG family) in the presence of a host of environmental and system uncertainty can be found in Ref. [1]. Six-degree-of-freedom Monte Carlo simulation performance of A^{2}PDG law is reported in Ref. [11]. An evaluation of the performance of the Apollo lunar descent guidance (another important member of the FP^{2}DG family) in powered descent in atmosphere can be found in Ref. [12].

C. Trajectory Shaping in Lunar Landing

The differences among various trajectories in Section V-B should be taken in the context that the powered descent time is only 100 sec in a Mars landing mission. For a lunar landing mission where there is no atmosphere to help slow down the vehicle, the powered descent time will be much longer, [10] and the trajectory differences are expected to be more pronounced. Because of such a long descent flight, the lunar descent trajectory may still need to be divided into phases as in the Apollo landing where 3 phases are used: braking phase, approach phase, and terminal descent phase. [3] In the Apollo program the powered descent trajectory in each phase is shaped by choosing the appropriate targeting condition for the trajectory in that phase (i. e., $\boldsymbol{r}_f^*$ and $\boldsymbol{V}_f^*$ in Eqs. (3) and (4) and $\boldsymbol{a}_{T_f}^*$; but the trajectory in a phase terminates before actually reaching the targeting condition to avoid the singularity of the guidance at $t_{go} = 0$). The fractional-polynomial powered descent guidance laws developed herein provide additional more direct and substantial trajectory shaping options by adjusting one or both scalar parameters k_r and γ in Eq. (62).

VI. Conclusions

Fifty years after the historical lunar landing by Apollo 11, there is a strong renewed interest in human return to the Moon. It is timely and befitting that a theory of fractional-polynomial powered descent guidance (FP^{2}DG) is developed in this paper to bring a new perspective to one of the technological innovations of the Apollo program, the Apollo powered descent guidance technology exemplified by Apollo lunar descent guidance and E-guidance laws. In this paradigm a family of powered descent guidance laws are obtained from a unique approach of tracking control with a particular fractional-polynomial based reference thrust acceleration profile. This family of guidance laws are defined by a single equation with two user-tunable parameters. An equivalence theory developed in this work helps reveal that each member of this family is actually an *explicit* guidance law derivable from a thrust acceleration profile defined by another fractional polynomial. This insight explains why these guidance laws behave in a predictable fashion and the targeting accuracy is always good. The Apollo lunar descent guidance and E-guidance laws are shown to be two members of this large family of fractional-polynomial guidance laws. As such, we have discovered numerous siblings of the Apollo lunar descent guidance and E-guidance laws, each offering a different trajectory with varying thrust characteristics, but all enjoying similar strengths in simplicity and excellent targeting performance. This new found flexibility in trajectory and guidance command shaping, not available with Apollo lunar descent guidance and E-guidance laws, could prove valuable in the new quest for lunar landing capability as well as the exploration of other planets. As a final complement an automated closed-loop targeting technique is developed to support the guidance method to avoid a possible singularity near the end of the trajectory.

Acknowledgments

This research has been supported by NASA Grant 80NSSC19M0119. The author thanks the anonymous reviewers for this paper whose comments and suggestions have helped improve the presentation.

Appendix:: Derivation of Beyond-Termination Targeting Condition

By Proposition 2, FP^{2}DG law in Eq. (43) is equivalent to the explicit guidance law

$$\boldsymbol{a}_T(t_{go}) = \boldsymbol{a}_{T_f} + \boldsymbol{c}_1 t_{go}^{\gamma_1} + \boldsymbol{c}_2 \tau_{go}^{\gamma_2}, \quad \gamma_1 = \gamma > 0, \gamma_2 = \frac{k_r}{\gamma + 2} - 2 \tag{A.1}$$

where $\boldsymbol{a}^*_{T_f}$ in Eq. (43) has been replaced by the to-be-determined $\boldsymbol{a}_{T_f}$. Denote

$$\phi_i = t_{go}^{\gamma_i}, \bar{\phi}_i = -\frac{1}{\gamma_i + 1} t_{go}^{\gamma_i + 1}, \hat{\phi}_i = \frac{1}{(\gamma_i + 1)(\gamma_i + 2)} t_{go}^{\gamma_i + 2}, \quad i = 1, 2 \tag{A.2}$$

$$\phi_i^* = \Delta t_{go}^{\gamma_i}, \bar{\phi}_i^* = -\frac{1}{\gamma_i + 1} \Delta t_{go}^{\gamma_i + 1}, \hat{\phi}_i^* = \frac{1}{(\gamma_i + 1)(\gamma_i + 2)} \Delta t_{go}^{\gamma_i + 2}, \quad i = 1, 2 \tag{A.3}$$

where $t_{go} \geq \Delta t_{go} \geq 0$. For any such a t_{go} the state solutions corresponding to the thrust profile in Eq. (A.1) are

$$\boldsymbol{r}(t_{go}) = \boldsymbol{r}_f + \boldsymbol{c}_1 \hat{\phi}_1 + \boldsymbol{c}_2 \hat{\phi}_2 - \boldsymbol{V}_f t_{go} + \frac{1}{2}\left(\boldsymbol{g} + \boldsymbol{a}_{T_f}\right) t_{go}^2 \tag{A.4}$$

$$\boldsymbol{V}(t_{go}) = \boldsymbol{V}_f + \boldsymbol{c}_1 \bar{\phi}_1 + \boldsymbol{c}_2 \bar{\phi}_2 - \left(\boldsymbol{g} + \boldsymbol{a}_{T_f}\right) t_{go} \tag{A.5}$$

where $\boldsymbol{r}_f$ and $\boldsymbol{V}_f$ are the final radius and velocity vectors. To start from the current state ($\boldsymbol{r}$, $\boldsymbol{V}$) at $t_{go} > 0$ and end at ($\boldsymbol{r}_f$, $\boldsymbol{V}_f$) at $t_{go} = 0$, the coefficients $\boldsymbol{c}_1$ and $\boldsymbol{c}_2$ are given, much like in Eqs. (31) and (32), as the following

$$\boldsymbol{c}_1 = \frac{-\hat{\phi}_2\left[\boldsymbol{V} - \boldsymbol{V}_f + \left(\boldsymbol{g} + \boldsymbol{a}_{T_f}\right) t_{go}\right] + \bar{\phi}_2\left[\boldsymbol{r} - \boldsymbol{r}_f + \boldsymbol{V}_f t_{go} - \frac{1}{2}\left(\boldsymbol{g} + \boldsymbol{a}_{T_f}\right) t_{go}^2\right]}{\Delta} \tag{A.6}$$

$$c_2 = \frac{\hat{\phi}_1\left[\boldsymbol{V} - \boldsymbol{V}_f + \left(\boldsymbol{g} + \boldsymbol{a}_{T_f}\right)t_{go}\right] - \bar{\phi}_1\left[\boldsymbol{r} - \boldsymbol{r}_f + \boldsymbol{V}_f t_{go} - \frac{1}{2}\left(\boldsymbol{g} + \boldsymbol{a}_{T_f}\right)t_{go}^2\right]}{\Delta} \tag{A.7}$$

where Δ is the same as defined in Eq. (9). The above equations can be further expressed as

$$\boldsymbol{c}_1 = k_{1r}\boldsymbol{r}_f + k_{1V}\boldsymbol{V}_f + k_{1a}\boldsymbol{a}_{T_f} + \boldsymbol{d}_1 \tag{A.8}$$

$$\boldsymbol{c}_2 = k_{2r}\boldsymbol{r}_f + k_{2V}\boldsymbol{V}_f + k_{2a}\boldsymbol{a}_{T_f} + \boldsymbol{d}_2 \tag{A.9}$$

where

$$k_{1r} = -\frac{1}{\Delta}\bar{\phi}_2 \tag{A.10}$$

$$k_{1V} = \frac{1}{\Delta}\left(\bar{\phi}_2 t_{go} + \hat{\phi}_2\right) \tag{A.11}$$

$$k_{1a} = -\frac{1}{\Delta}\left(\frac{1}{2}\bar{\phi}_2 t_{go} + \hat{\phi}_2\right)t_{go} \tag{A.12}$$

$$k_{2r} = \frac{1}{\Delta}\bar{\phi}_1 \tag{A.13}$$

$$k_{2V} = -\frac{1}{\Delta}\left(\bar{\phi}_1 t_{go} + \hat{\phi}_1\right) \tag{A.14}$$

$$k_{2a} = -\frac{1}{\Delta}\left(\frac{1}{2}\bar{\phi}_1 t_{go} + \hat{\phi}_1\right)t_{go} \tag{A.15}$$

$$\boldsymbol{d}_1 = \frac{1}{\Delta}\left[\left(\boldsymbol{r} - \frac{1}{2}\boldsymbol{g}t_{go}^2\right)\bar{\phi}_2 - \left(\boldsymbol{V} + \boldsymbol{g}t_{go}\right)\hat{\phi}_2\right] \tag{A.16}$$

$$\boldsymbol{d}_2 = \frac{1}{\Delta}\left[\left(\boldsymbol{r} - \frac{1}{2}\boldsymbol{g}t_{go}^2\right)\bar{\phi}_1 - \left(\boldsymbol{V} + \boldsymbol{g}t_{go}\right)\hat{\phi}_1\right] \tag{A.17}$$

We require the radius, velocity, and thrust acceleration vectors in Eqs. (A.4), (A.5) and (A.1) at the specified instant $t_{go} = \Delta t_{go}$ to be $\boldsymbol{r}_f^*$, $\boldsymbol{V}_f^*$, and $\boldsymbol{a}_{T_f}^*$, respectively, that is,

$$\boldsymbol{r}_f^* = \boldsymbol{r}_f + \boldsymbol{c}_1\hat{\phi}_1^* + \boldsymbol{c}_2\hat{\phi}_2^* - \boldsymbol{V}_f\Delta t_{go} + \frac{1}{2}\left(\boldsymbol{g} + \boldsymbol{a}_{T_f}\right)\Delta t_{go}^2 \tag{A.18}$$

$$\boldsymbol{V}_f^* = \boldsymbol{V}_f + \boldsymbol{c}_1\bar{\phi}_1^* + \boldsymbol{c}_2\bar{\phi}_2^* - \left(\boldsymbol{g} + \boldsymbol{a}_{T_f}\right)\Delta t_{go} \tag{A.19}$$

$$\boldsymbol{a}_{T_f}^* = \boldsymbol{a}_{T_f} + \boldsymbol{c}_1\phi_1^* + \boldsymbol{c}_2\phi_2^* \tag{A.20}$$

Using $\boldsymbol{c}_1$ and $\boldsymbol{c}_2$ in Eqs. (A.8) and (A.9) in Eqs. (A.18)–(A.20), and collecting the like terms, we have

$$\boldsymbol{r}_f^* = m_{11}\boldsymbol{r}_f + m_{12}\boldsymbol{V}_f + m_{13}\boldsymbol{a}_{T_f} + \boldsymbol{b}_1 \tag{A.21}$$

$$\boldsymbol{V}_f^* = m_{21}\boldsymbol{r}_f + m_{22}\boldsymbol{V}_f + m_{23}\boldsymbol{a}_{T_f} + \boldsymbol{b}_2 \tag{A.22}$$

$$\boldsymbol{a}_{T_f}^* = m_{31}\boldsymbol{r}_f + m_{32}\boldsymbol{V}_f + m_{33}\boldsymbol{a}_{T_f} + \boldsymbol{b}_3 \tag{A.23}$$

where

$$m_{11} = k_{1r}\hat{\phi}_1^* + k_{2r}\hat{\phi}_2^* + 1 \tag{A.24}$$

$$m_{12} = k_{1V}\hat{\phi}_1^* + k_{2V}\hat{\phi}_2^* - \Delta t_{go}^2 \tag{A.25}$$

$$m_{13} = k_{1a}\hat{\phi}_1^* + k_{2a}\hat{\phi}_2^* + \frac{1}{2}\Delta t_{go}^2 \tag{A.26}$$

$$m_{21} = k_{1r}\bar{\phi}_1^* + k_{2r}\bar{\phi}_2^* \tag{A.27}$$

$$m_{22} = k_{1V}\bar{\phi}_1^* + k_{2V}\bar{\phi}_2^* + 1 \tag{A.28}$$

$$m_{23} = k_{1a}\bar{\phi}_1^* + k_{2a}\bar{\phi}_2^* - \Delta t_{go}^2 \tag{A.29}$$

$$m_{31} = k_{1r}\phi_1^* + k_{2r}\phi_2^* \tag{A.30}$$

$$m_{32} = k_{1V}\phi_1^* + k_{2V}\phi_2^* \tag{A.31}$$

$$m_{33} = k_{1a}\phi_1^* + k_{2a}\phi_2^* + 1 \tag{A.32}$$

and

$$\boldsymbol{b}_1 = \hat{\phi}_1^* \boldsymbol{d}_1 + \hat{\phi}_2^* \boldsymbol{d}_2 + \frac{1}{2} \boldsymbol{g} \Delta t_{go}^2 \tag{A.33}$$

$$\boldsymbol{b}_2 = \bar{\phi}_1^* \boldsymbol{d}_1 + \bar{\phi}_2^* \boldsymbol{d}_2 - \boldsymbol{g} \Delta t_{go} \tag{A.34}$$

$$\boldsymbol{b}_3 = \phi_1^* \boldsymbol{d}_1 + \phi_2^* \boldsymbol{d}_2 \tag{A.35}$$

From these definitions it is evident that m_{ij}'s are functions of t_{go} and Δt_{go} only, and $\boldsymbol{b}_i$'s are functions of $\boldsymbol{r}$, $\boldsymbol{V}$, t_{go} and Δt_{go}. The solution to the linear algebraic system in Eqs. (A.21)–(A.23) may be put in a compact form of

$$\begin{bmatrix} \boldsymbol{r}_f \\ \boldsymbol{V}_f \\ \boldsymbol{a}_{T_f} \end{bmatrix} = M^{-1} \left\{ \begin{bmatrix} \boldsymbol{r}_f^* \\ \boldsymbol{V}_f^* \\ \boldsymbol{a}_{T_f}^* \end{bmatrix} - \boldsymbol{b} \right\} \tag{A.36}$$

where $M \in R^{9 \times 9}$ and $\boldsymbol{b} \in R^9$ are defined by

$$M = \begin{bmatrix} m_{11}\boldsymbol{I}_3 & m_{12}\boldsymbol{I}_3 & m_{13}\boldsymbol{I}_3 \\ m_{21}\boldsymbol{I}_3 & m_{22}\boldsymbol{I}_3 & m_{21}\boldsymbol{I}_3 \\ m_{31}\boldsymbol{I}_3 & m_{32}\boldsymbol{I}_3 & m_{33}\boldsymbol{I}_3 \end{bmatrix}, \quad \boldsymbol{b} = \begin{bmatrix} \boldsymbol{b}_1 \\ \boldsymbol{b}_2 \\ \boldsymbol{b}_3 \end{bmatrix} \tag{A.37}$$

with I_3 being the 3 × 3 identity matrix.

It can be verified that the matrix M in Eq. (A.37) has full rank, thus invertible, for any $\gamma_2 > 0$, $t_{go} > 0$, and $t_{go} > \Delta t_{go} \geq 0$. In particular when $\Delta t_{go} = 0$, M reduces to an identity matrix and $\boldsymbol{b} = 0$ for any $t_{go} > 0$, thus the solution from Eq. (A.36) is $\left(\boldsymbol{r}_f, \boldsymbol{V}_f, \boldsymbol{a}_{T_f}\right) = \left(\boldsymbol{r}_f^*, \boldsymbol{V}_T^*, \boldsymbol{a}_{T_f}^*\right)$ as expected, because this is the case where no beyond-termination targeting is done. For a given $\Delta t_{go} > 0$ the targeting equation in Eq. (A.36) is evaluated in each guidance cycle along the trajectory using the current state ($\boldsymbol{r}(t)$, $\boldsymbol{V}(t)$) (on which $\boldsymbol{b}$ is dependent) and the current t_{go}. The thrust acceleration command is then generated from Eq. (43), except that ($\boldsymbol{r}_f^*$, $\boldsymbol{V}_f^*$, $\boldsymbol{a}_{T_f}^*$) in Eq. (43) is now replaced by ($\boldsymbol{r}_f$, $\boldsymbol{V}_f$, $\boldsymbol{a}_{T_f}$). But the update of ($\boldsymbol{r}_f$, $\boldsymbol{V}_f$, $\boldsymbol{a}_{T_f}$) should stop as t_{go} gets close to Δt_{go}, to avoid numerical singularity of M (and there is no practical benefit to continue to update the targeting condition as the trajectory is near the end).

A degenerate case is when $\gamma_2 = 0$, i. e., $k_r = 2(\gamma + 2)$ in the FP^{2}DG law. In this case the parameterization of the thrust acceleration profile in Eq. (A.1) loses 3 degrees-of-freedom, and the matrix M only has a rank of 6. Not all the components of the targeting condition triplet ($\boldsymbol{r}_f^*$, $\boldsymbol{V}_f^*$, $\boldsymbol{a}_{T_f}^*$) at the actual guidance termination can be satisfied. In such a case only ($\boldsymbol{r}_f^*$, $\boldsymbol{V}_f^*$) will be enforced by choosing ($\boldsymbol{r}_f$, $\boldsymbol{V}_f$). Define $M_{sub} \in R^{6 \times 6}$ and $\boldsymbol{b}_{sub} \in R^6$ by

$$M_{sub} = \begin{bmatrix} m_{11}\boldsymbol{I}_3 & m_{12}\boldsymbol{I}_3 \\ m_{21}\boldsymbol{I}_3 & m_{22}\boldsymbol{I}_3 \end{bmatrix}, \boldsymbol{b}_{sub} = \begin{bmatrix} \boldsymbol{b}_1 \\ \boldsymbol{b}_2 \end{bmatrix} \tag{A.38}$$

The targeting condition at the beyond-termination point is then

$$\begin{bmatrix} \boldsymbol{r}_f \\ \boldsymbol{V}_f \end{bmatrix} = M_{sub}^{-1}\left\{\begin{bmatrix} \boldsymbol{r}_f^* \\ \boldsymbol{V}_f^* \end{bmatrix} - \boldsymbol{b}_{sub}\right\} \tag{A.39}$$

Another case of caution is $k_r = (\gamma + 2)^2$ where $\gamma_2 = \gamma_1 = \gamma$. In this case $\Delta \equiv 0$ by Eq. (9). Therefore the parameters in Eqs. (A.10)–(A.17) are undefined, and the numerical solution based on the implementation of these equations will not be obtainable. For this particular choice of k_r, the proposed beyond-termination targeting should not be done.

Nomenclature

A²PDG	Augmented Apollo Powered Descent Guidance
$\mathbf{a_d}$	reference thrust acceleration vector in R^3 (m/s^2)
$\mathbf{a_T}$	commanded thrust acceleration vector in R^3 (m/s^2)
$\boldsymbol{a}_{T_f}^*$	desired final thrust acceleration vector in R^3 (m/s^2)
$\boldsymbol{c}_0, \boldsymbol{c}_1, \boldsymbol{c}_2$	coefficient vectors in R^3
FP²DG	Fractional-Polynomial Powered Descent Guidance
$\mathbf{g}$	planetary gravitational acceleration vector in R^3 (m/s^2)
$\boldsymbol{k_r}, \boldsymbol{k_V}$	constant feedback gains
PDI	Powered Descent Initiation
$\mathbf{r}$	position vector in R^3 (m)
$\mathbf{r_d}$	reference position vector in R^3 (m)
$\boldsymbol{r}_f^*$	specified final position vector in R^3 (m)
$\mathbf{t}$	current time (s)
$\mathbf{t_f}$	specified final time (s)
$\mathbf{t_{go}}$	time-to-go ($t_f - t$) (s)
$\mathbf{V}$	velocity vector in R^3 (m/s)
$\mathbf{V_d}$	reference velocity vector in R^3 (m/s)
$\boldsymbol{V}_f^*$	specified final velocity vector in R^3 (m/s)

$\boldsymbol{\beta_r(t_{go})}$	position feedback gain function (1/s^2)
$\boldsymbol{\beta_V(t_{go})}$	velocity feedback gain function (1/s)
$\boldsymbol{\phi_1(t_{go}), \phi_2(t_{go})}$	basis functions
$\bar{\phi}_1(t_{go}), \bar{\phi}_2(t_{go})$	integrals of ϕ_1 and ϕ_2
$\hat{\phi}_1(t_{go}), \hat{\phi}_2(t_{go})$	integrals of $\bar{\phi}_1$ and $\bar{\phi}_2$
$\boldsymbol{\gamma, \gamma_1, \gamma_2}$	positive real numbers
$\boldsymbol{\Delta}$	$\hat{\phi}_1(t_{go})\bar{\phi}_2(t_{go}) - \hat{\phi}_2(t_{go})\bar{\phi}_1(t_{go})$
$\boldsymbol{\Delta t_{go}}$	a short time interval beyond actual guidance termination (s)

References

[1]. Lu P, “Augmented Apollo Powered Descent Guidance,” Journal of Guidance, Control, and Dynamics, Vol. 42, No. 3, 2019, pp. 447–457. doi:10.2514/1.G004048.

[2]. Cherry GW, “A General, Explicit, Optimizing Guidance Law for Rocket-Propelled Spaceflight,” AIAA Paper 64–638, 1964. doi:10.2514/6.1964-638.

[3]. Klumpp AR, “Apollo Lunar-Descent Guidance,” MIT Charles Stark Draper Laboratory Report R-695, 1971.

[4]. Klumpp AR, “Apollo Lunar Descent Guidance,” Automatica, Vol. 10, No. 2, 1974, pp. 133–146. doi:10.1016/0005-1098(74)90019-3.

[5]. Royston P and Altman DG, “Regression using Fractional Polynomials of Continuous Covariates: Parsimonious Parametric Modelling,” Applied Statistics, Vol. 43, No. 3, 1994, pp. 429–467.

[6]. Royston P and Sauerbrei W, Multivariable Model-Building: A Pragmatic Approach to Regression Analysis based on Fractional Polynomials for Modelling Continuous Variables, chap. 4, John Wiley & Sons, New York, 2008.

[7]. Cerimele C, Robertson E, Sostaric R, Campbell C, Robinson P, Matz D, Johnson B, and Stachowiak S, “A Rigid Mid Lift-to-Drag Ratio Approach to Human Mars Entry, Descent, and Landing,” AIAA Paper 2017–1898, 2017. doi:10.2514/6.2017-1898.

[8]. Lu P, “Entry Guidance: a Unified Method,” Journal of Guidance, Control, and Dynamics, Vol. 37, No. 3, 2014, pp. 713–728. doi:10.2514/1.62605.

[9]. D’Souza CS, “An Optimal Guidance Law for Planetary Landing,” AIAA Paper 97–3709, 1997. doi:10.2514/6.1997-3709.

[10]. Bennett FV, “Apollo Lunar Descent and Ascent Trajectories,” NASA TM X-58040, 1970.

[11]. Johnson BJ, Lu P, and Cerimele CJ, “Mid-Lift-to-Drag ratio Rigid Vehicle 6-DoF EDL Performance Using Tunable Apollo Powered Descent Guidance,” AAS/AIAA Astrodynamics Specialist Conference, Portland, ME, AAS Paper 19–619, 2019.

[12]. Strohl LD, An Evaluation of Apollo Powered Descent Guidance, Master’s thesis, San Diego State University, 2018.

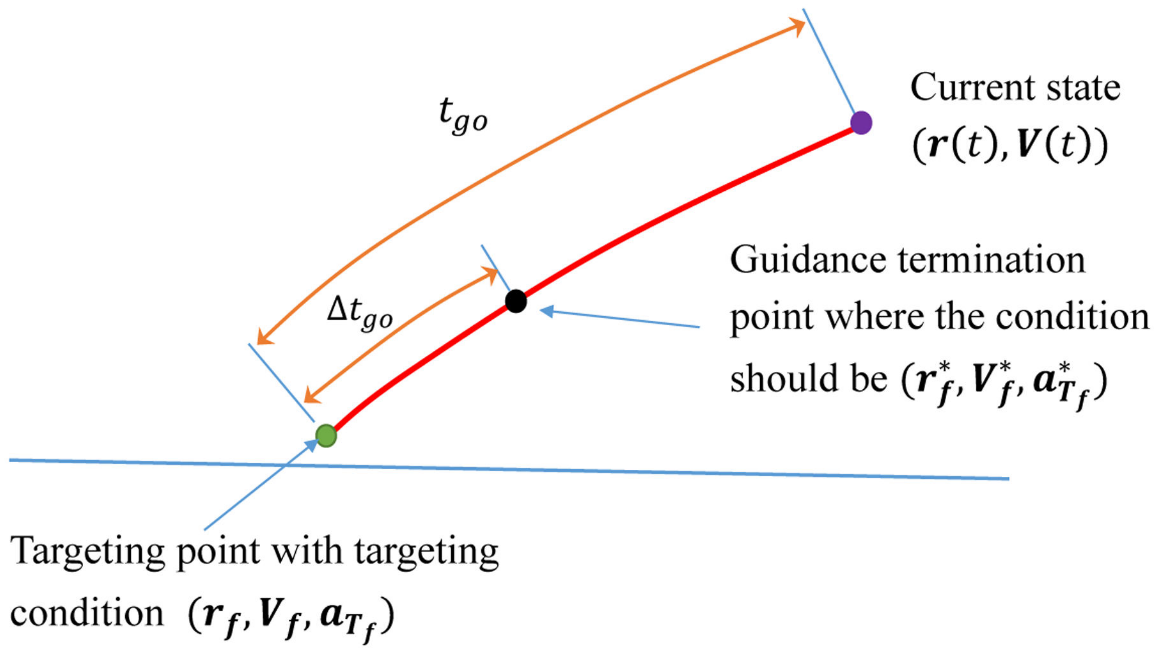

Figure 1.

Illustration of beyond-termination targeting

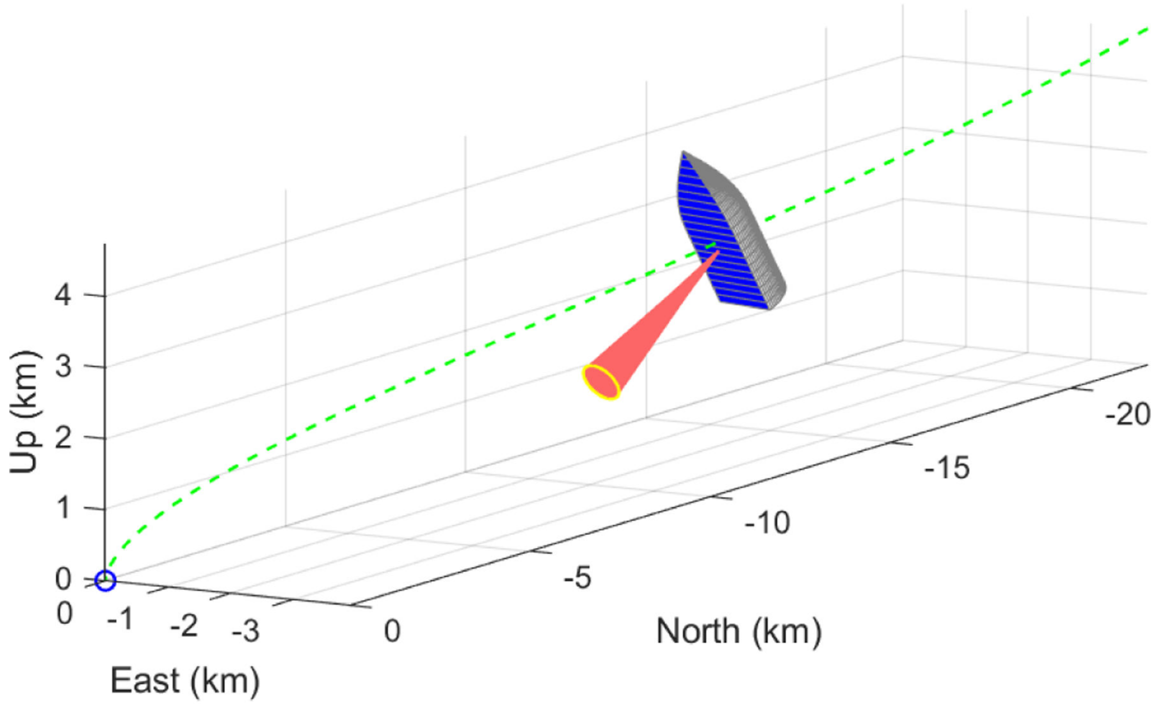

Figure 2.
A mid L/D vehicle in powered descent (the red cone indicates the direction of the thrust vector)

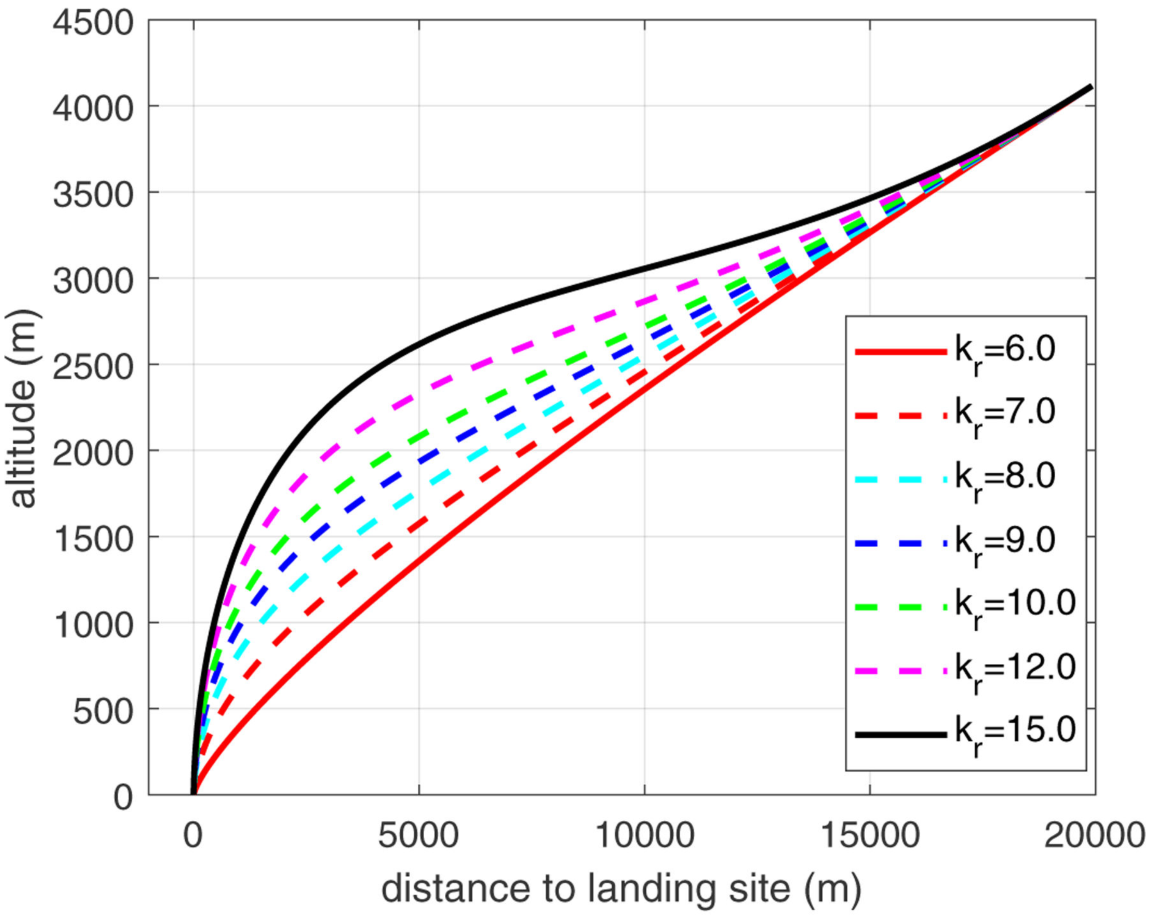

Figure 3.
Powered descent trajectories under tunable guidance law in Eq. (62) with $\gamma = 1$ (i. e., Eq. (64)) for different values of k_r

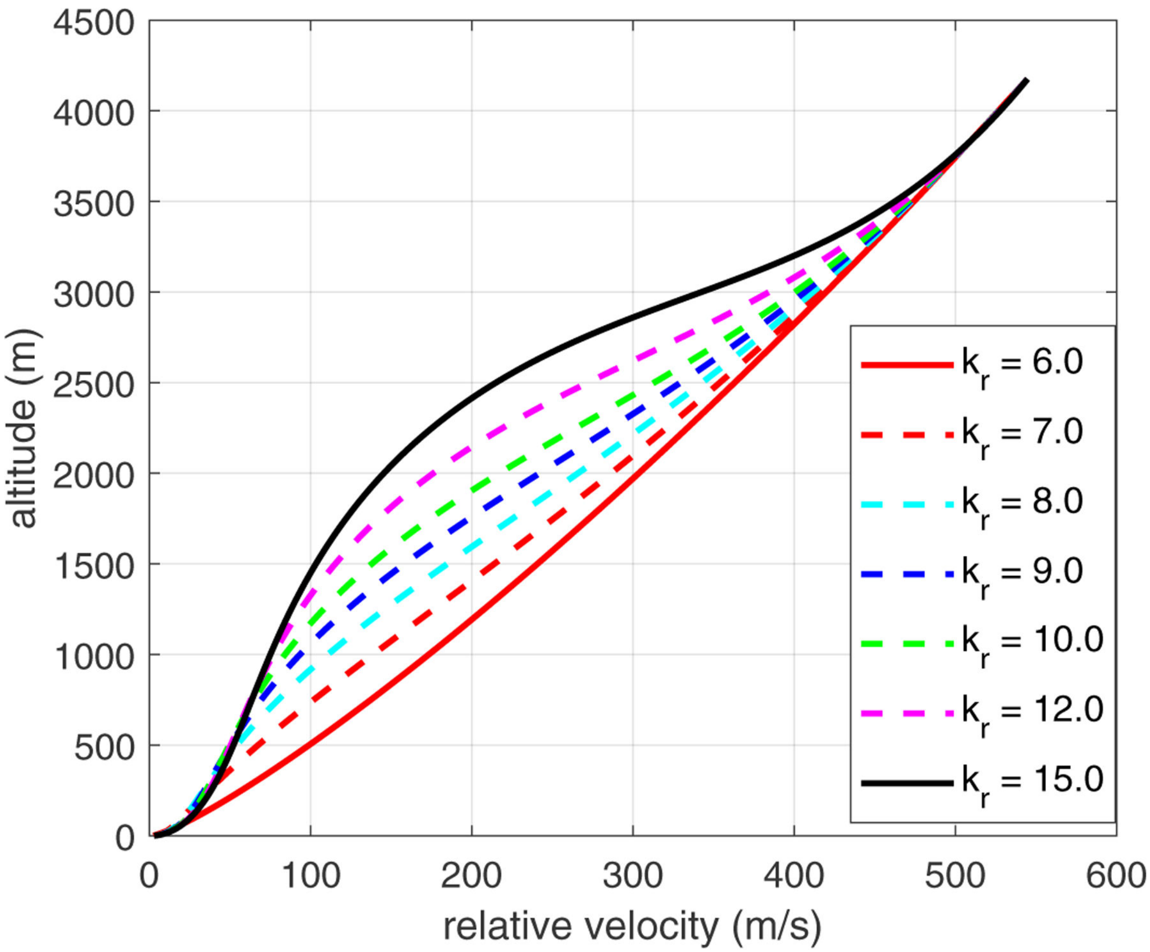

Figure 4.

Variations of altitude versus velocity under tunable guidance law in Eq. (62) with $\gamma = 1$ (i.e., Eq. (64)) for different values of k_r

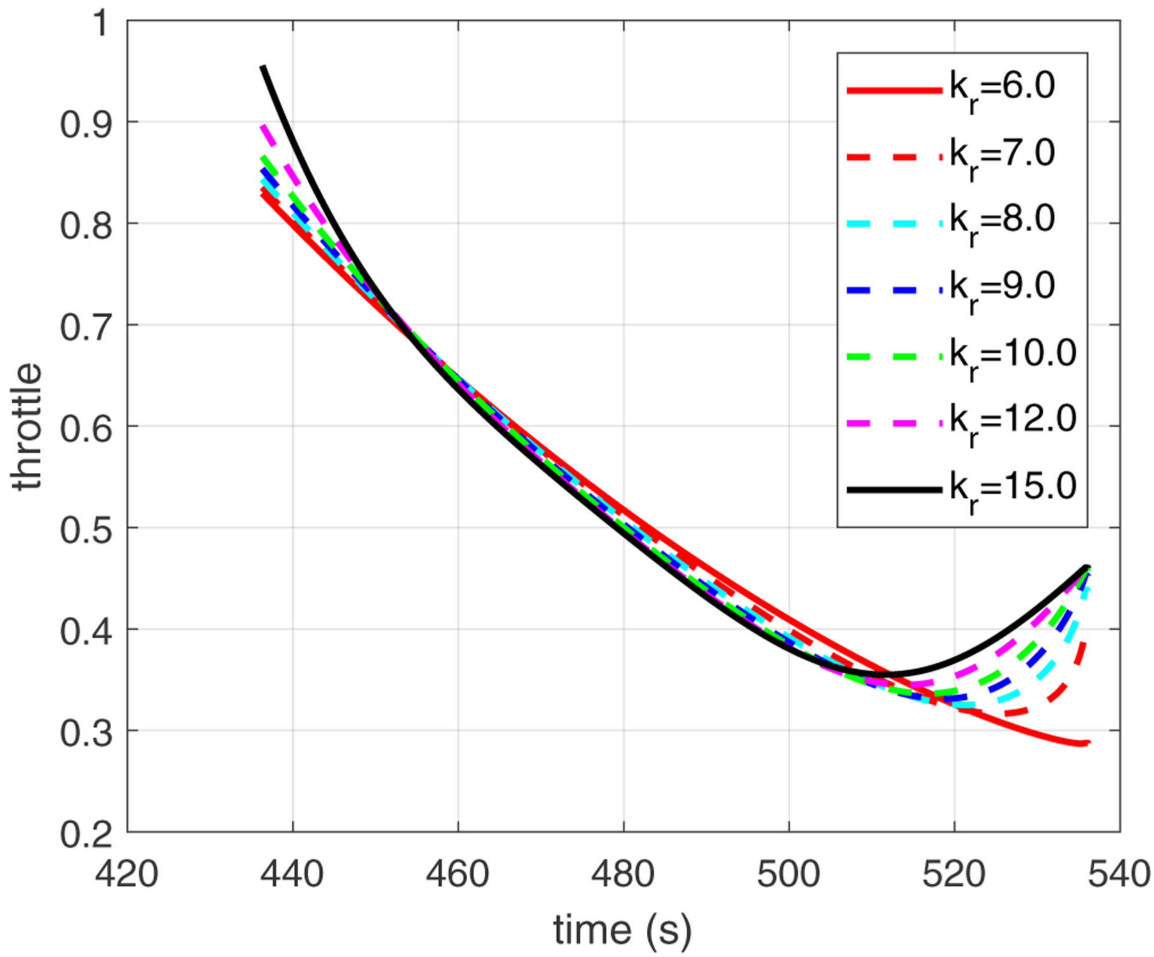

Figure 5.

Engine throttle settings under tunable guidance law in Eq. (62) with $\gamma = 1$ (i. e., Eq. (64)) for different values of k_r

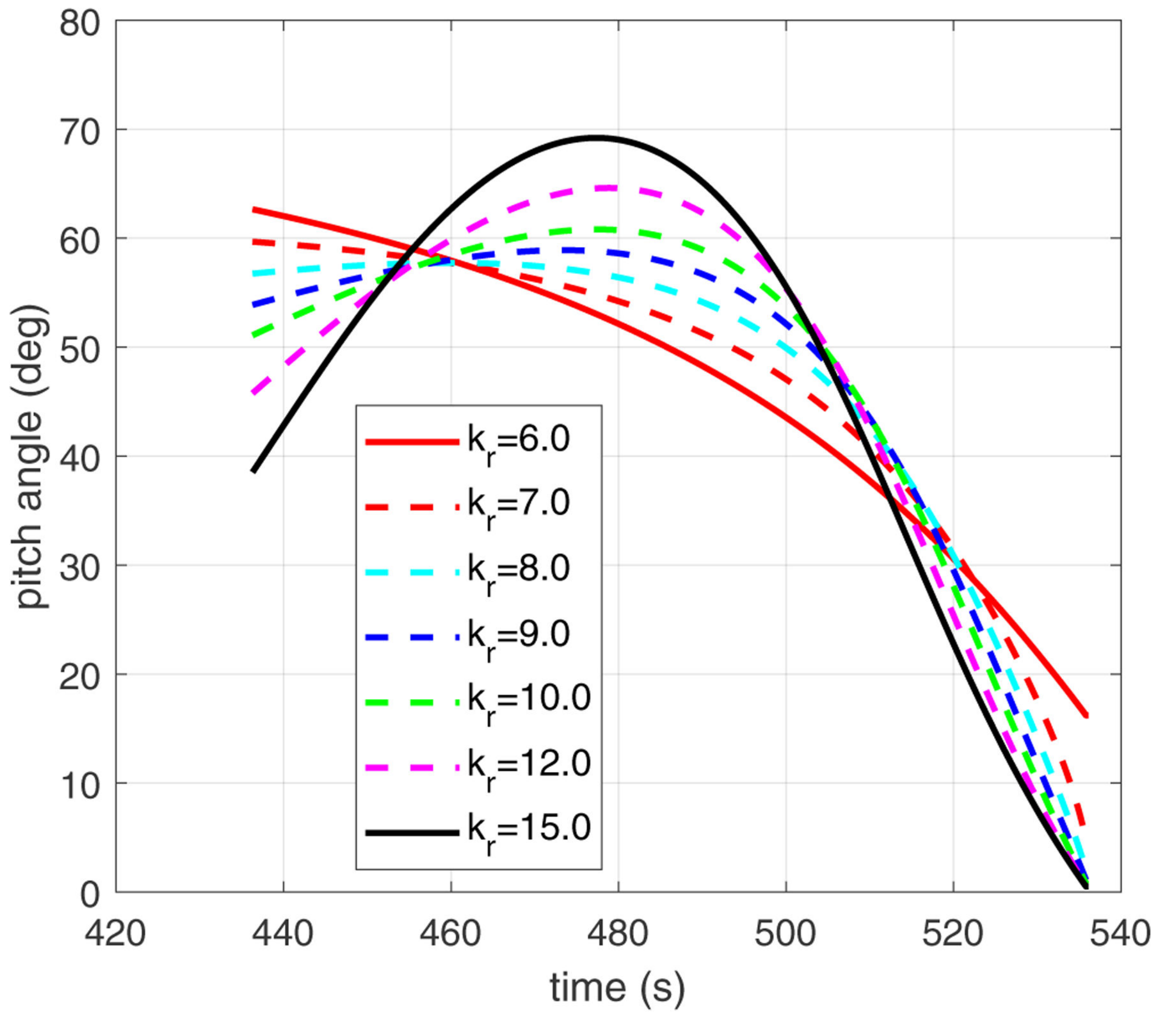

Figure 6.

Pitch angle profiles of the vehicle with respect to the NED frame under the tunable guidance law in Eq. (62) with $\gamma = 1$ (i. e., Eq. (64)) for different values of k_r

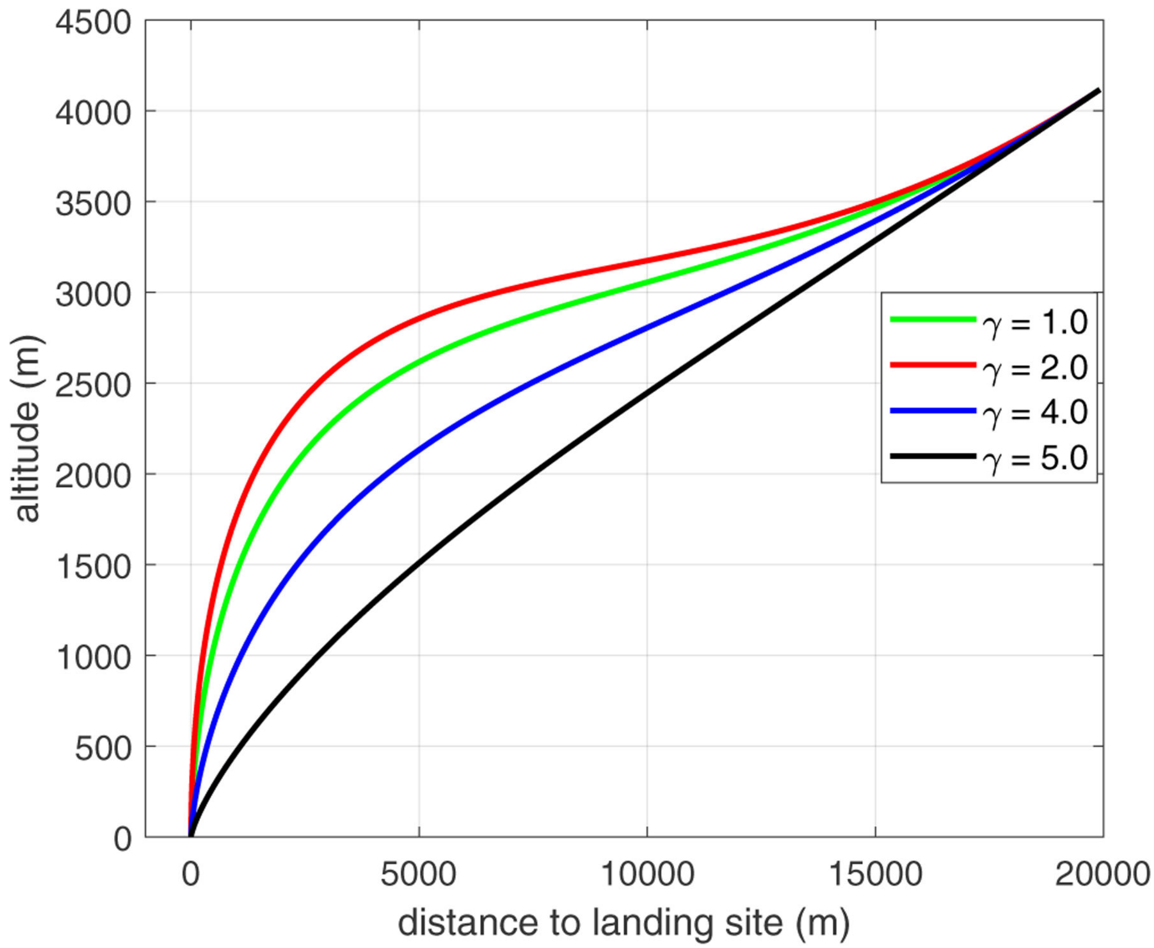

Figure 7.

Powered descent trajectories under tunable guidance law in Eq. (62) with $k_r = 15$ for different values of γ

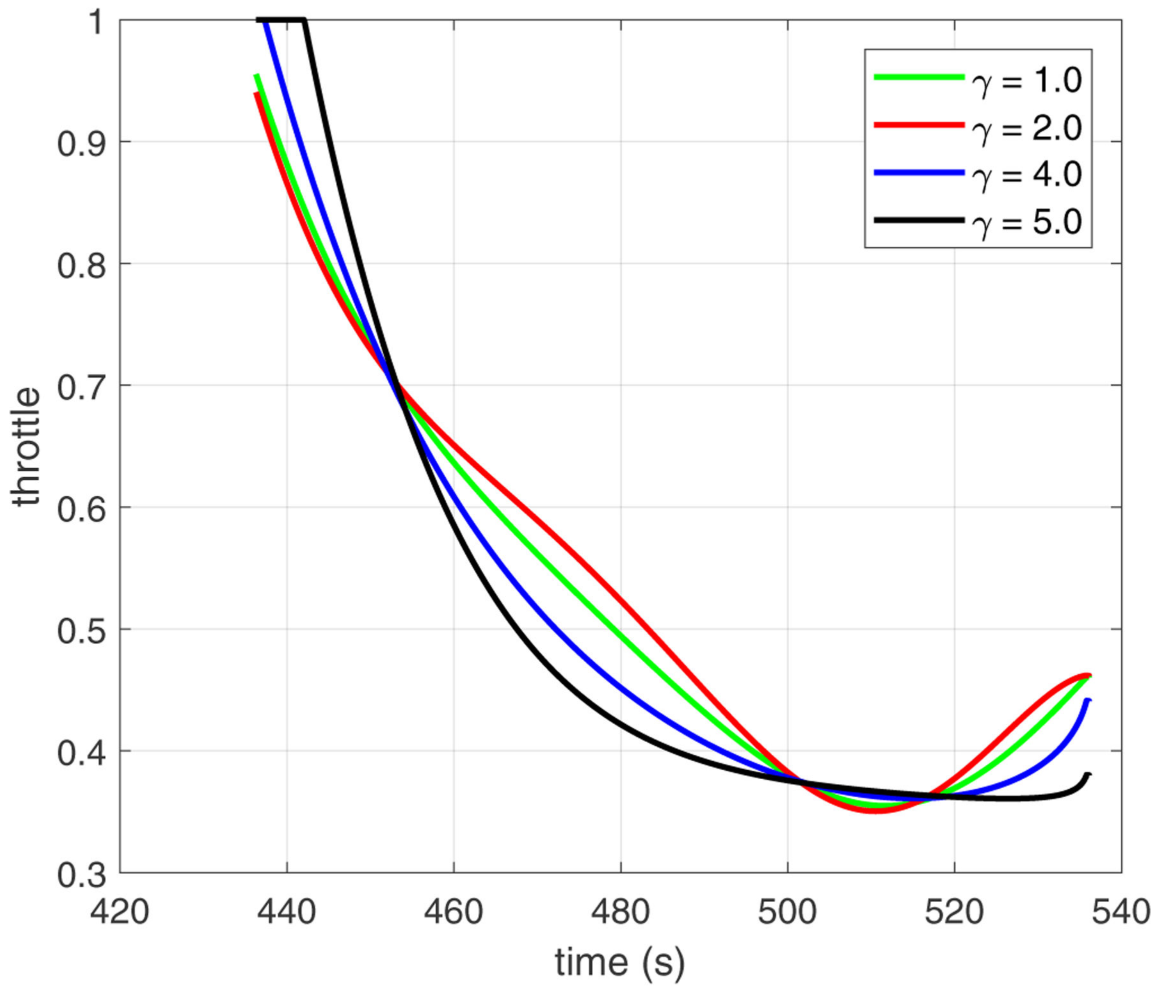

Figure 8.
Throttle settings under tunable guidance law in Eq. (62) with $k_r = 15$ for different values of γ

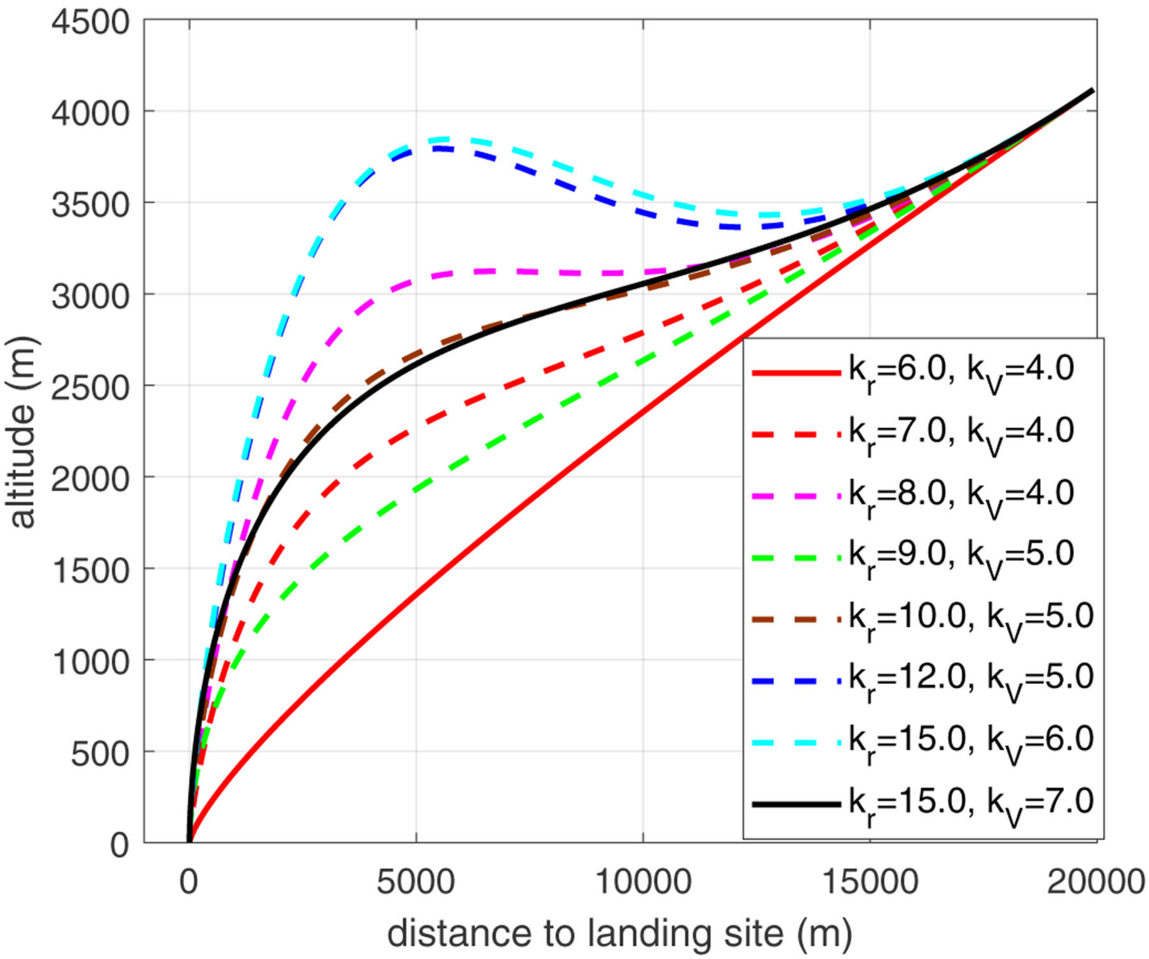

Figure 9.

Trajectories under tracking guidance law in Eq. (68) with $\gamma = 1$ for different values of k_r and k_V. They are sporadic.

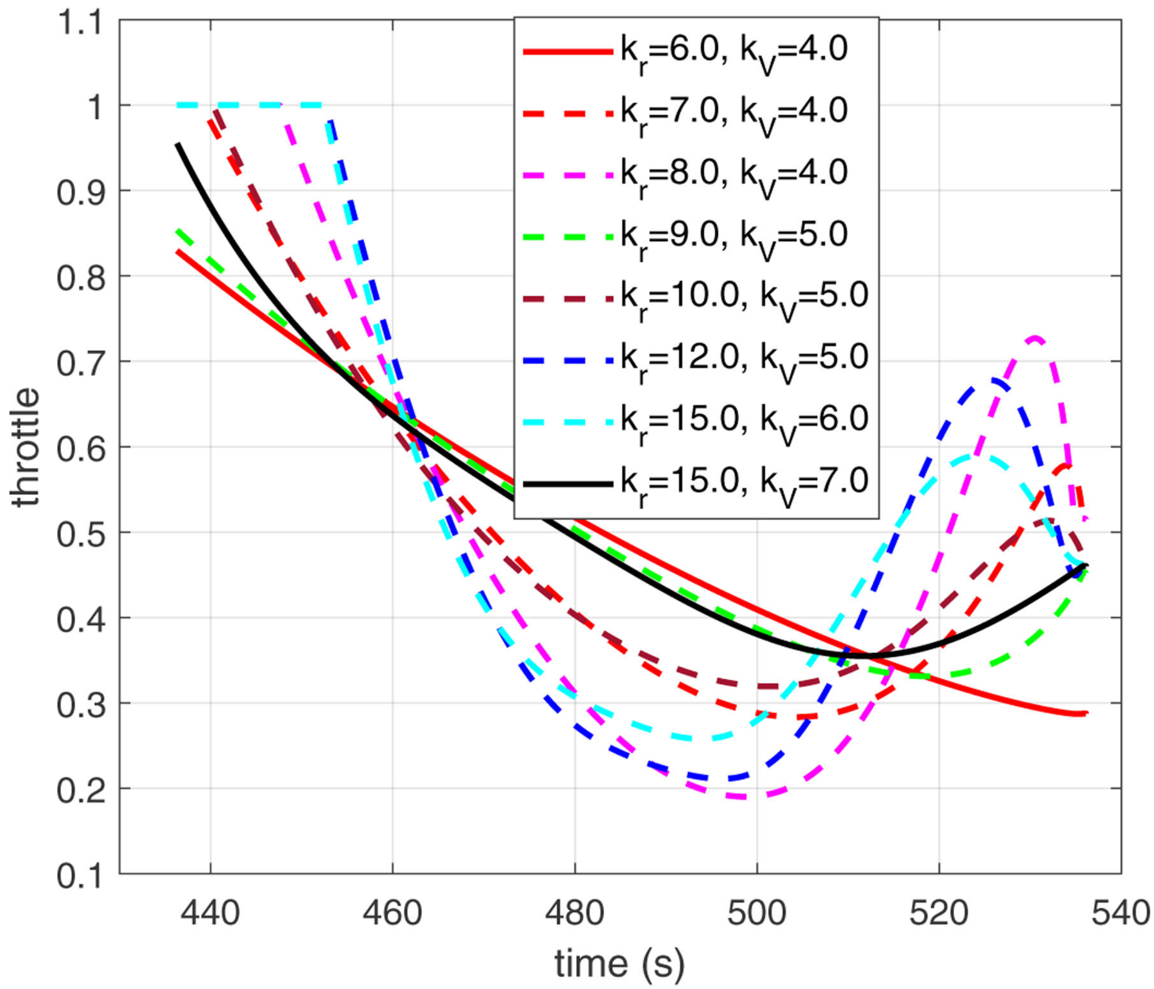

Figure 10.

Engine throttle settings under tracking guidance law in Eq. (68) with $\gamma = 1$ for different values of k_r and k_V

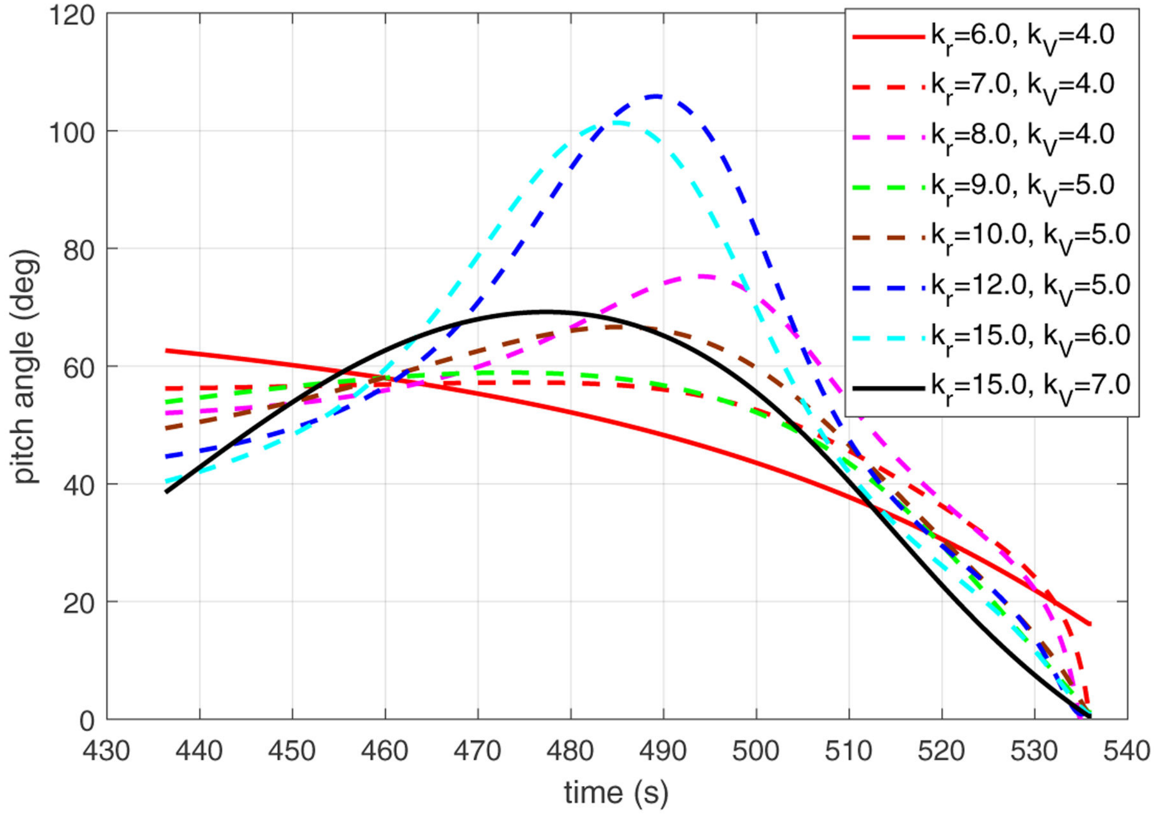

Figure 11.

Pitch angle of the vehicle with respect to the NED frame under tracking guidance law in Eq. (68) with $\gamma = 1$ for different values of k_r and k_V. They are volatile.

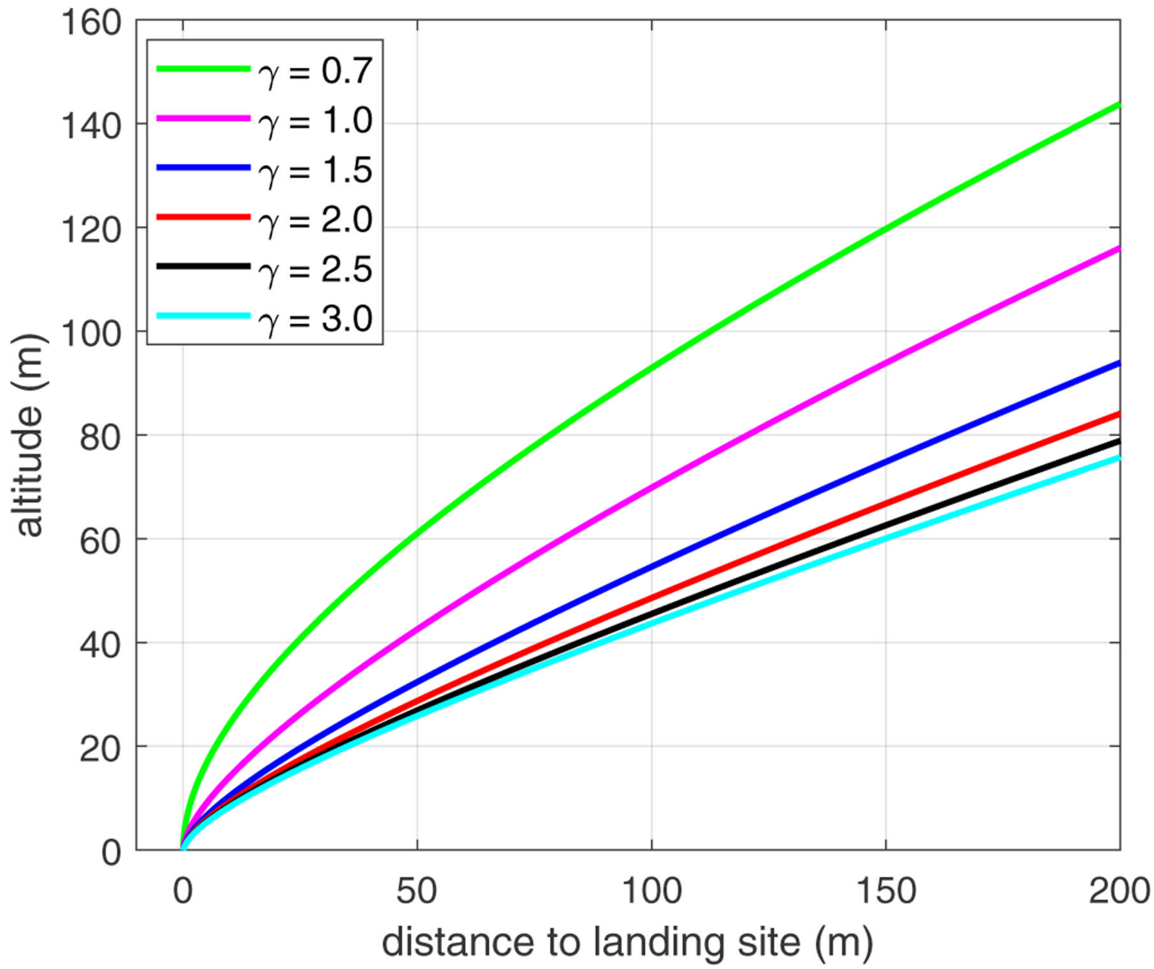

Figure 12.
Trajectories under guidance law in Eq. (62) with $k_r = 2(\gamma + 2)$ (i. e., Eq. (66)) for different values of γ

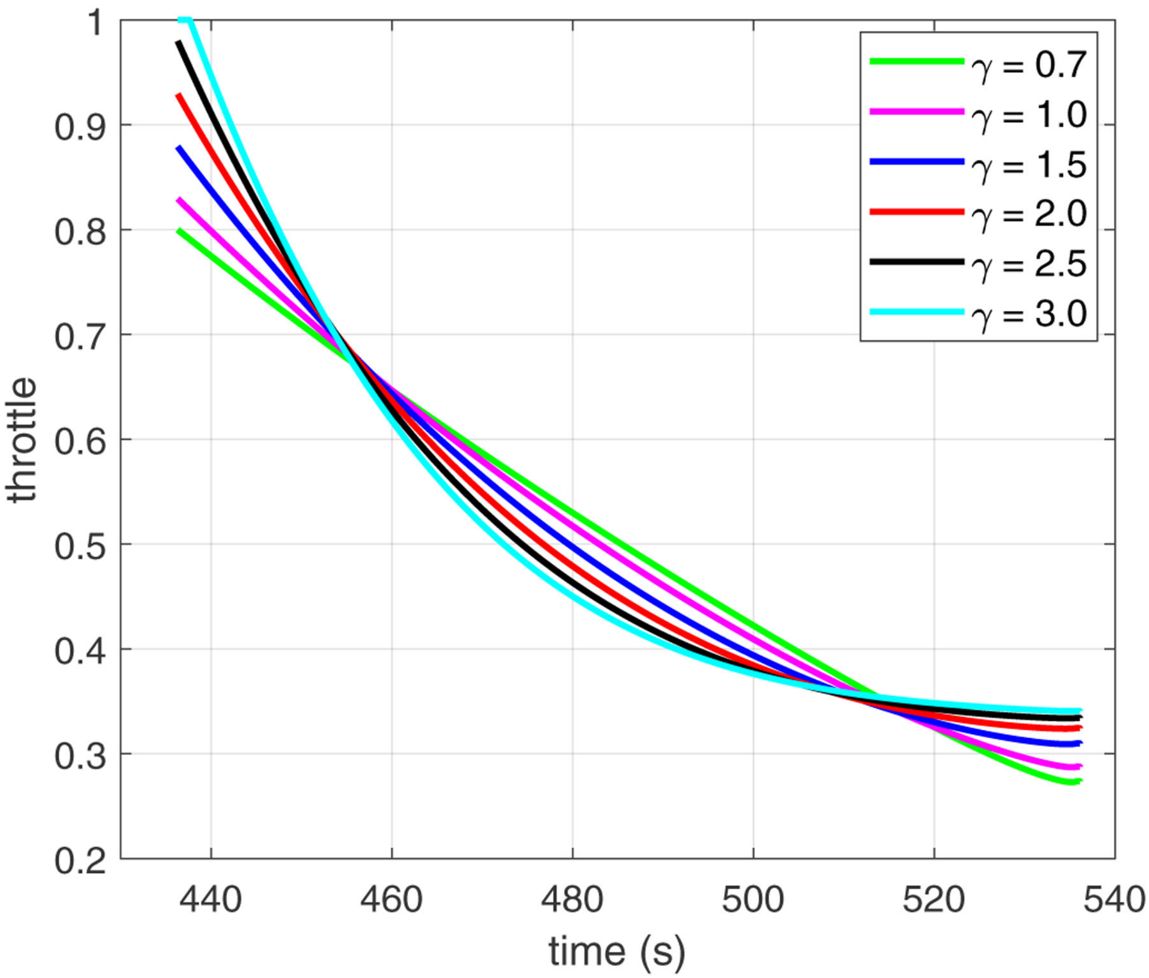

Figure 13.

Engine throttle settings under guidance law in Eq. (62) with $k_r = 2(\gamma + 2)$ (i. e., Eq. (66)) for different values of γ

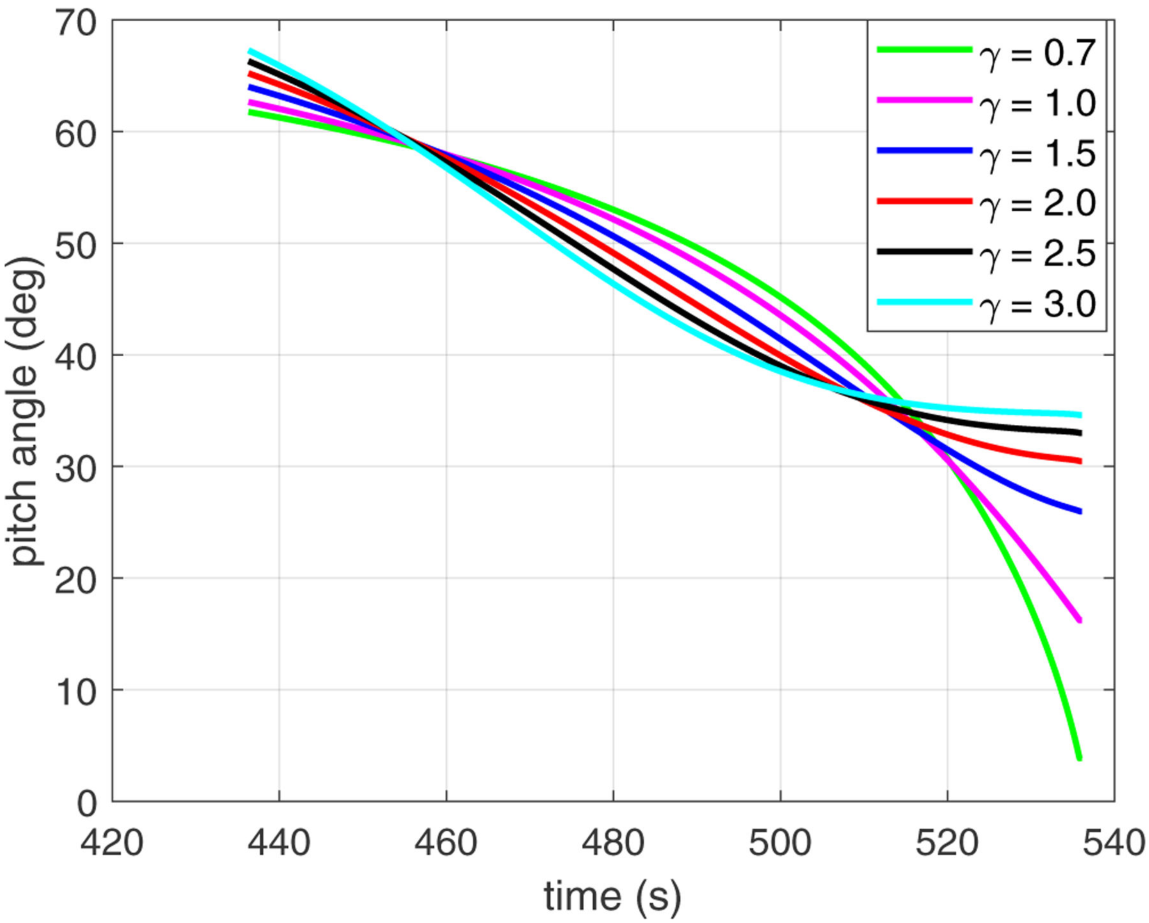

Figure 14.

Pitch angle profiles with respect to the NED frame under guidance law in Eq. (62) with $k_r = 2(\gamma + 2)$ (i. e., Eq. (66)) for different values of γ

NASA Author Manuscript
NASA Author Manuscript